Agricultural Water Management 303 (2024) 109028

Contents lists available at ScienceDirect

Agricultural Water Management

journal homepage: www.elsevier.com/locate/agwat

Simulation of source sink partitioning in wheat under varying nitrogen regimes using DSSAT-CERES-wheat model

Mukhtar Ahmed[a,b,*], Muhammad Bilal[a], Shakeel Ahmad[c]

[a] Department of Agronomy, Pir Mehr Ali Shah Arid Agriculture University, Rawalpindi 46300, Pakistan
[b] Swedish University of Agricultural Sciences, Umea, Sweden
[c] Department of Agronomy, Bahauddin Zakariya University, Multan 60800, Pakistan

ARTICLE INFO

Handling Editor: J.E. Fernández

Keywords:
DSSAT_CERES_Wheat
Radiation use efficiency
Phenology
Yield
Water use efficiency

ABSTRACT

Grain yields in wheat can be limited by the assimilate supply (source) or by the carbohydrate demand of the grains (sink). Recently, there have been questions regarding the capability of crop models to simulate the physiology of source-sink interactions in crops; however, crop models scarcely tested with source-sink partitioning. DSSAT_CERES_Wheat model was used with details of field experimental data having treatments of manipulated source (i.e., assimilate supply), sink (i.e., kernel number). The aim of the present study was to assess the impact of different levels of nitrogen and source-sink manipulation on wheat crop and to model source-sink partitioning in wheat under varying N-Regimes and climatic conditions. The experiment was conducted during wheat growing seasons of 2015–16 and 2016–17, at two locations (Islamabad and URF Koont Chakwal), under five different levels of nitrogen and three source sink treatments (Control (100 % RUE), 50 % shading pre-anthesis (50 % RUE), 50 % spike removal i.e. spike halving) using randomized complete block design. Recommended rates of fertilizer were applied with the exception of nitrogen which was 0, 50, 100, 150 and 200 kg ha^{-1}, while each treatment was replicated thrice. CERES-Wheat model was calibrated using 2015–16 observed data while model was evaluated using two-year field collected data of two sites i.e. Islamabad and Chakwal. The model was able to simulate treatments impacts on phenology (R^2, RMSE and d-index values of 0.89, 2.80 days and 0.97 respectively at Islamabad while at Chakwal $R^2 = 0.89$, RMSE = 2.65 days and d-index = 0.94), leaf area index ($R^2 = 0.94$, 0.94, RMSE = 0.51, 0.38 and d-index = 0.98 and 0.92 at Islamabad and Chakwal respectively), biomass ($R^2 = 0.98$, 0.96, RMSE = 370, 450 kg ha^{-1} and d-index = 0.96 and 0.95 at Islamabad and Chakwal respectively), grain yield ($R^2 = 0.97$,0.96, RMSE = 0.17, 0.2 t ha^{-1}, and d-index = 0.95 and 0.93 at Islamabad and Chakwal respectively), harvest index, soil nitrogen, crop nitrogen and grain nitrogen with good accuracy. The observed range for biomass water use efficiency (BM_WUE) was 34.1–14.5 kg ha^{-1} mm^{-1} while grain WUE remained in the range of 10.3–3.7 kg ha^{-1} mm^{-1}. The results depicted that model could reproduce observed effects of shading and halving the spikes. Crop response to modified radiation use efficiency (RUE) was variable among sites which could be critical for studying crop environment interactions, improving WUE, estimating genetically and atmospheric CO_2-related increased RUE, analyzing impact of solar dimming and source manipulations under biotic stress.

1. Introduction

The current climate scenario presents new challenges to worlds rising population. Food security is one of the big future challenge. Food security closely relates to climate change (Ahmed, 2023; Guarin et al., 2022; Lee et al., 2024). Climate change and food security mitigation are major issues for agriculture in developing countries. The human population is expected to increase from 7.2 to 9.8 billion in 2050 and 11.2 billion in 2100 which represent population increase of 35 %. However, demand for agricultural products will increase by about 70 % in the same period to meet the global standard of living. Therefore, accurate sustainable production of most widely grown crop i.e. wheat is needed to fulfill the food demand as it is fulfilling 21 % of the world's food requirements (Deng et al., 2021; Shewry and Hey, 2015). This task is challenging as maintaining wheat production will be difficult in some regions due to decreasing solar radiation (Gu et al., 2017; Yang et al.,

* Corresponding author at: Department of Agronomy, Pir Mehr Ali Shah Arid Agriculture University, Rawalpindi 46300, Pakistan.
E-mail address: ahmadmukhtar@uaar.edu.pk (M. Ahmed).

https://doi.org/10.1016/j.agwat.2024.109028
Received 22 February 2024; Received in revised form 19 August 2024; Accepted 22 August 2024
Available online 28 August 2024
0378-3774/© 2024 The Author(s). Published by Elsevier B.V. This is an open access article under the CC BY license (http://creativecommons.org/licenses/by/4.0/).

2013) and increasing temperature (Ahmed, 2020; Asseng et al., 2015; Fatima et al., 2020; IPCC, 2023; Kheir et al., 2019). The substantial increase in wheat yield during green revolution was due to introduction and amendments of dwarf cultivars and nitrogen fertilizers. Similarly, higher yield and harvest index in latest wheat cultivars were because of increased number of grains per unit area. Yet, in last few decades yield stagnation was observed. Therefore, the next quantum leap in wheat crop yield is possible by higher biomass production combined with optimization of source-sink ratio (Bustos et al., 2013). Significant impact of sink development and source capacity under heat and drought stress have been reported on grain yield and quality of wheat (Mohan et al., 2023; Zahra et al., 2021). Earlier researchers suggested improvement in the dynamic interactions of both storage and photosynthetic processes to improve grain yield and quality (Ponsioen et al., 2007; Reynolds et al., 2007). Source and sink strengths also have significant influence on the rate and amount of dry matter accumulation and growth of harvestable organs. However, these strengths vary during the main growth phases of the crop and alterations in source-sink balance during these phases can affect growth, yield and yield components (Asseng et al., 2017).

Source-sink limitation timing has specific impacts as reduced source between booting and anthesis will not influence the number of spikelet initiated on a spike. Similarly, crop sensitive stages such as stem elongation and shortly after flowering have critical effect on wheat yield (Dreccer et al., 2018). Ferrante et al., (2013) concluded that floret primordia have been initiated when the flag leaf completed growth. Floret development is critical for grain setting in wheat, but it has been reported that 50 % of grain yield potential is lost during stem elongation phase if environmental and agronomic conditions are not suitable. However, if environment and management interactions are ideal then extending the duration of this phase resulted to higher yields because of increased number of fertile florets at anthesis (Guo et al., 2018).This also influences assimilate allocation to the spike and to other plant parts. Thus, source limitation before anthesis will reduce the number of grains per unit area. Alonso et al., (2018) highlighted that under ideal conditions grain yield in wheat is highly associated with sink capacity. Source and sink have established dynamic interactions but understanding of this interaction under different biomass growth scenarios is compulsory to have improve future grain yields.

The regulation of biomass production and assimilate translocation in plants can be controlled by source-sink relation. Alteration in source-sink ratio has shown impact on seed dry weight but source–sink manipulations during the seed filling period was more effective. It has been demonstrated quantitatively that yield is usually more sink than source limited during grain filling (Borrás et al., 2004a; Cartelle et al., 2006; Serrago et al., 2013). Furthermore, modification in source-sink ratio during seed filling resulted to changes in stem dry weight. This showed that stem reserves act as a buffer between the photo-assimilates produced and sink demand. Changes in stem elongation is an important way to increase spike dry weight at anthesis as it guarantee an adequate supply of assimilate for grain filling after anthesis (González et al., 2011, 2003; Schnyder, 1993). However, C4 crops such as maize are highly inefficient in the use of assimilates stored before flowering for sink growth as compared to C3 crops like wheat. Conversion efficiency of pre-flowering photo-assimilates to grain biomass in maize was 0.26 g of seed g^{-1} while in wheat it was 0.68–0.78 g of seed g^{-1} (Gebbing et al., 1999; Kiniry et al., 1992).This exhibited that modification in source before flowering in wheat will produce more significant impacts on grain growth. The amount of dry matter accumulation and growth rate of the harvested parts of crop is determined by source-sink strength (Asseng et al., 2016). Optimizing biomass production joined with source-sink ratio would prominently increase grain yield of wheat (Bustos et al., 2013; Miralles and Slafer, 2007a; Miralles et al., 2007; Slafer and Savin, 1994; Sun et al., 2009). As to grain development there is considerable confirmation that sink limit is a real constraining element for harvest efficiency (Reynolds et al., 2005). Borrill et al. (2015) documented that potential yield gains due to delayed leaf senescence should be linked with increased sink capacity. Similarly, Zhang et al., (2010) suggested that wheat yield is more sink than source limited therefore to lift the yield potential of wheat larger sink size should be considered.

Crop simulation models are valuable tool widely applied in agronomic studies and designing of adaptation options under changing climate (Afzal et al., 2024; Ahmed et al., 2024a, b; Ahmed et al., 2023; Amouzou et al., 2018; Dueri et al., 2022; Galmarini et al., 2024; Jahan et al., 2018; Kimball et al., 2023; Naz et al., 2024). Most commonly used models such as CERES (Ritchie et al., 1998), STICS (Artru et al., 2018; Rafique et al., 2024) and NWheat (Asseng et al., 2017) considers kernel number as the main determinant of yield formation. These models use empirical relationships and coefficients to determine kernel number based on growth before anthesis. Generally, grain yield in a crop model are simulated as function of kernel numbers per unit area and availability of assimilates. Thus, these models are source-sink co limited. Modeling was used to find the simplest way of evaluating the genotype, environment and management (G × E × M) interactions (Cooper and Hammer, 1996). Crop predicting models are powerful tools used broadly for the analysis of crop growth and cropping systems (Matthews et al., 2013; White et al., 2011). Modeling trials in different rainfed regions showed the significance of remobilization for crop yield (Asseng and Van Herwaarden, 2003). Previous studies revealed that simulation models could successfully simulate all growth and development factors of crop (Asseng et al., 2001). Environmental changes like increasing temperature and higher concentration of atmospheric CO_2 affects source-sink relations (Uddling et al., 2008). Therefore, evaluation of crop models is necessary to study source-sink philosophy under wide range of managements and environmental scenarios. The hypothesis of this study was how source sink manipulation under different levels of N can impact wheat crop phenology, biomass, yield and WUE under rainfed conditions and can DSSAT_ CERES-Wheat model has potential to simulate the impact of source sink manipulation in response to varying N regimes. Hence main aim of this study was to test the potential of DSSAT_CERES-Wheat model under variable rainfed sites of Pothwar to predict wheat crop phenology, leaf area index (LAI), biomass, yield, crop N and grain N by using measured field data of nitrogen and source sink manipulations i.e. source-reduction (shading) and sink reduction (Spike halving at anthesis).

2. Materials and methods

2.1. Field experiments

For evaluation of nitrogen fertilization and source sink partitioning in wheat through DSSAT_CERES-Wheat model, crop and soil data were collected from field experiments during two wheat growing seasons (2015–16 and 2016–17) at University Research Farm Koont (URFK) Chakwal (32.93° N, 72.86° E) and National Agriculture Research Center (NARC) Islamabad (38.78° N, 73.57° E) having an altitude of 525 m and 540 m above sea level respectively (Fig. 1). University Research Farm Koont (URFK) is 15 Km away from Chakwal which is low rainfall site of rainfed Pothwar. In these experiments a spring wheat cultivar Pak-2013 was sown on 10th November in lines with row-to-row distance of 30 cm. The seed rate used was 120 kg ha^{-1}. The previous crop grown in field before wheat sowing was soybean at both sites. Soil samples were taken before crop sowing to determine the various physio-chemical properties of experimental soil as well as initial soil water content. Detail analysis of soil as proposed by International Benchmark Sites Network for Agrotechnology Transfer (IBSNAT (1988) have been shown in Table 1 that was used to calibrate and evaluate DSSAT model. Furthermore, initial field conditions before the start of DSSAT_CERES_Wheat simulations have been given in Table 2.

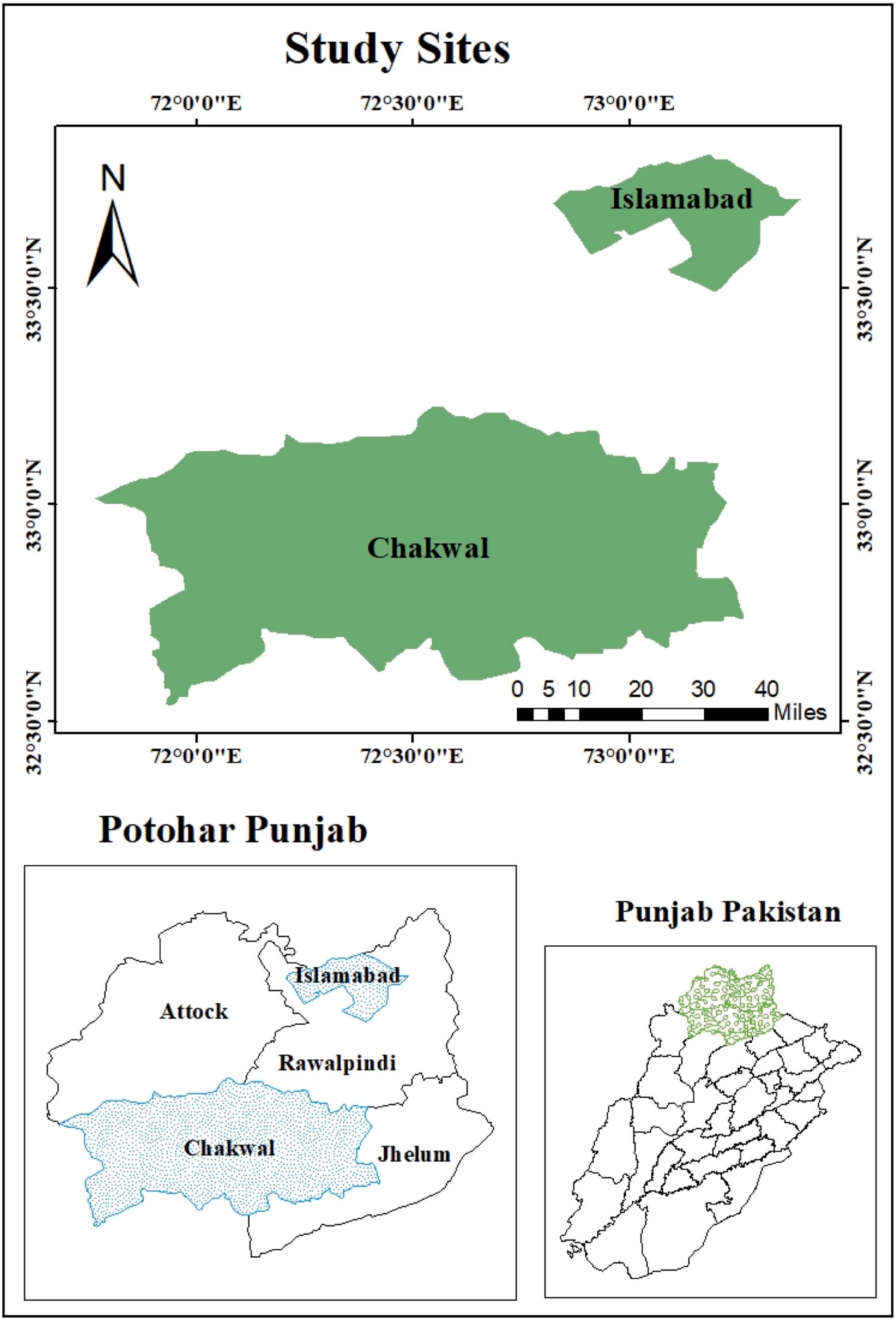

Fig. 1. Map of study sites.

Table 1
Physio-chemical properties of soil at two study sites.

Locations	Depth (cm)	SLLL (cm^3 cm^{-3})	SDUL (cm^3 cm^{-3})	SSAT	SRGF	SSKS (cm h^{-1})	SBDM (g cm^{-3})	SLOC (%)	SLCL (%)	SLSI (%)	SLHW
Islamabad	20	0.11	0.31	0.43	1	0.23	1.23	0.91	29	27	7.4
	40	0.12	0.26	0.41	0.55	0.43	1.3	0.89	30	25	7.5
	60	0.13	0.20	0.41	0.37	0.43	1.35	0.77	28	27	7.7
	80	0.10	0.24	0.42	0.25	1.32	1.46	0.59	25	29	8.1
	100	0.10	0.24	0.42	0.17	1.32	1.49	0.51	27	29	8.2
	120	0.10	0.24	0.42	0.11	0.23	1.57	0.38	28	30	8.2
	140	0.10	0.25	0.41	0.07	0.23	1.57	0.35	29	30	8.2
	160	0.10	0.25	0.41	0.05	1.32	1.58	0.31	26	32	8.2
URFK Chakwal	20	0.056	0.24	0.44	1	0.23	1.32	0.73	29	36	7.9
	40	0.063	0.20	0.41	0.55	0.23	1.47	0.68	31	35	8.1
	60	0.068	0.21	0.38	0.37	0.23	1.61	0.66	33	34	8.4
	80	0.068	0.23	0.33	0.25	0.23	1.67	0.54	35	32	8.3
	100	0.069	0.23	0.3	0.17	0.23	1.75	0.41	36	32	8.5
	120	0.077	0.22	0.26	0.11	0.23	1.75	0.32	35	33	8.7
	140	0.081	0.22	0.26	0.07	0.23	1.75	0.29	35	32	8.8
	160	0.081	0.22	0.24	0.05	0.23	1.86	0.26	36	34	8.8

Where SLLL: Soil lower limit, SDUL: Soil drain upper limit, SSAT: Soil saturation, soil root growth factor (SRGF), SSKS: Sat. hydraulic conductivity, macropore, cm h^{-1}, SBDM: Bulk density, moist, g cm^{-3}, SLOC: Soil organic carbon (SOC), SLCL: Clay (<0.002 mm) %, SLSI: Silt (0.05–0.002 mm) %,: SLHW: pH in water and URFK: University Research Farm Koont

Table 2
Initial field conditions before the start of DSSAT_CERES_Wheat Simulations.

Depth (cm) \Locations	Islamabad			Chakwal		
	SH_2O (cm^3 cm^{-3})	SNH_4 (mg kg^{-1})	SNO_3 (mg kg^{-1})	SH_2O (cm^3 cm^{-3})	SNH_4 (mg kg^{-1})	SNO_3 (mg kg^{-1})
20	0.31	3.6	6.0	0.22	2.7	4.0
40	0.32	3.6	6.0	0.21	2.7	4.0
60	0.33	3.6	5.0	0.20	2.7	3.0
80	0.33	3.3	4.0	0.20	2.6	3.0
100	0.33	3.2	3.0	0.20	2.5	3.0
120	0.33	3.1	2.0	0.20	2.4	2.0
140	0.33	3	0.5	0.20	2.1	0.5
160	0.33	3	0.5	0.20	1.0	0.5

Where SH_2O (cm^3 cm^{-3}): Initial field soil water, SNH_4 (mg kg^{-1}): soil ammonium N and SNO_3 (mg kg^{-1}): soil nitrate N

2.2. Modelling nitrogen fertilization, radiation use efficiency (RUE), shading impact and halving of spike

To model nitrogen fertilization (0, 50, 100, 150 and 200 kg N ha^{-1}) and source-sink treatments i.e. 100 % RUE, 50 % RUE (shading) and halving of spike impact on wheat crop phenology, leaf area index, biomass, grain weight, harvest index, soil nitrogen, crop nitrogen and grain nitrogen., experiment was laid out in RCBD (randomized complete block design) that was replicated thrice. Pictorial view of treatments has been shown in Fig. 2. Fifty percent RUE (shading) source-sink treatments was applied by covering the field with black net while in case of 100 % RUE plant was not covered with any material. Similarly, one side of spike was completely removed to set halving of spike treatment in field. There was a total of 45 treatments. Individual plot size was 2 m x 3 m, for treatment isolation 0.5 m plot to plot distance was maintained. Nitrogen treatments were applied at different levels as mentioned above in in the form of Urea (46 % N). Phosphorus was applied at the rate of 60 kg ha^{-1} to wheat crop at the time of seed bed preparation in the form of single super phosphate (SSP). Cultural practices were kept normal for wheat crop at both locations. Shading treatments to modify incident radiation were managed by covering the plots with black nets at 20 cm above the crop canopy.

2.3. Measurements of soil water and nitrogen dynamics

For gravimetric soil water determination, prior to sowing and at crop maturity when it was harvested layer wise (0–20,20–40, 40–60, 60–80, 80–100, 100–120, 120–140 and 140–160 cm) fresh soil samples were taken from each treatment plots using king tube. Fresh soil was transferred to the metallic cans and weighed by using digital balance. Afterwards samples were placed in an oven at 105° C until a constant dry weight of each sample was obtained. Then using following formula, soil water was recorded:

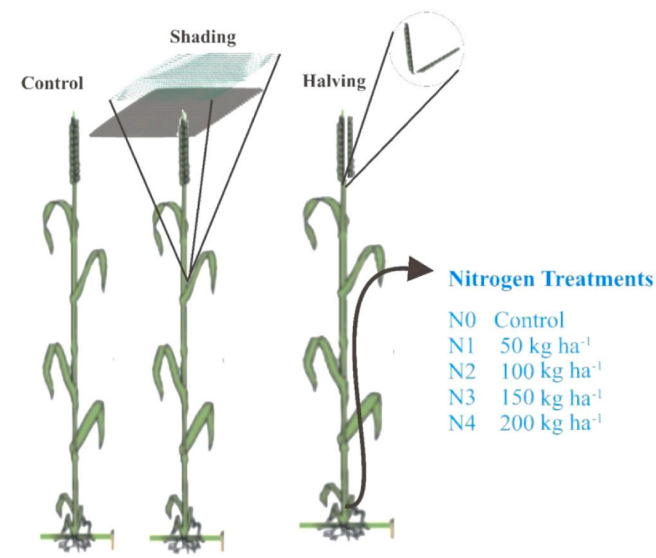

Fig. 2. Pictorial view of treatments i.e. nitrogen fertilization, 100 % RUE (Control), 50 % RUE (shading) and halving of spike.

$$\text{Gravimetric water}\left(\%\right) = \frac{\text{Fresh Soil weight} - \text{Oven dried soil weight}}{\text{Oven dried soil weight}} \times 100$$

Gravimetric water was afterwards converted to volumetric water by using following formulae:

$$Volumetric\ water(\%) = Gravimetricwater \times Bulk\ density\left(gcm^{-3}\right)$$

Finally, available water (mm) was calculated using following formulae:

$$Available\ water(mm) = (Volumetric\ water - Lower\ limit) \times \frac{Layer\ thickness}{10}$$

Nitrogen dynamics i.e. soil mineral N, crop and grain N was measured using standard protocol as described in International Center for Agricultural Research in the Dry Areas (ICARDA) soil manual. Soil mineral N (NH_4-N +NO_3-N) was determined by taking 25 g soil sample. Afterward 50 mL of distilled water were added into a 250 mL bottle for the determination of soil mineral N. This involves extraction with KCl, filtration of the extract, analysis by colorimetry, and conversion of nitrate and ammonium ppm to kg/ha based on bulk density of the soil.

At maturity, wheat plant samples from one-meter square area was used for the determination of crop and grain N. Nitrogen contents from plant samples were determined after oven drying at 65 °C for 48 hours. After drying, samples were ground using a Wiley Mill, and samples were placed in plastic bottles to determine N contents. Samples of 2 g in 30–50 mL of acid and approximately 100 mL sodium hydroxide (NaOH) solutions were used. The crop N was measured after wet digestion in concentrated sulphuric acid (H_2SO_4) using the Kjeldahl procedure. Similarly, grain N was determined using the Kjeldahl procedure.

2.4. Climate description

Data about climate variables i.e. daily minimum and maximum temperature (°C), rainfall (mm) were collected from Pakistan Meteorological Department (PMD). However solar radiation (Mj m^{-2} day^{-1}) was calculated using FAO method. The climate of Islamabad is dry sub-humid with >1000 mm average annual rainfall (high rainfall zone) and an average annual temperature of 21.3 °C while URFK Chakwal is situated in the medium rainfall zone with an average annual

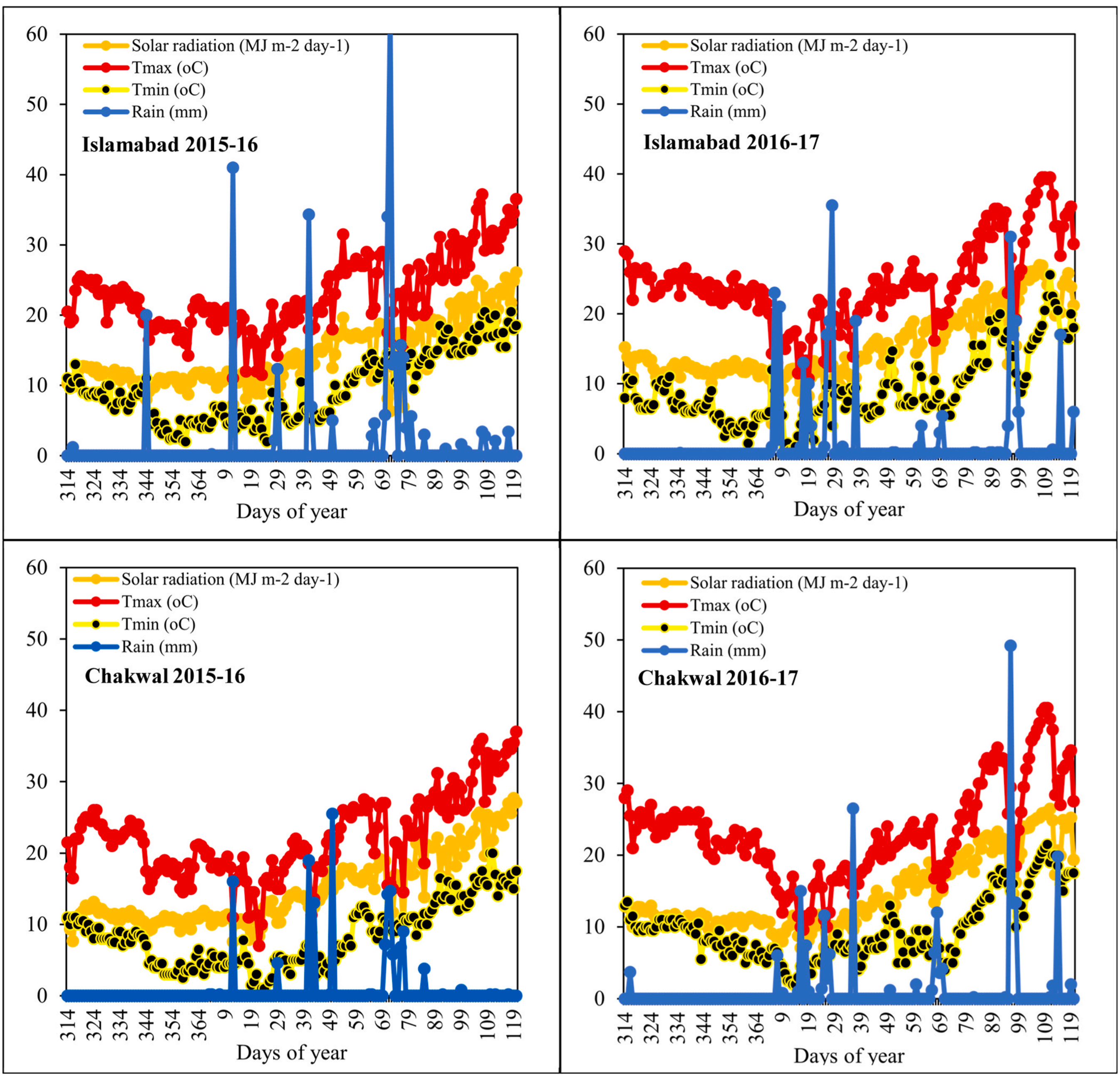

Fig. 3. Daily maximum and minimum temperatures (°C), rainfall (mm) and solar radiation (MJ m^{-2} day^{-1}) during 2015–16 and 2016–17 wheat growing season at study sites Islamabad and URFK Chakwal.

temperature of 22.4 °C (van Ogtrop et al., 2014). Weather conditions prevailed during both study seasons at two different study sites have been shown in Fig. 3.

2.5. CERES-wheat model

CERES-Wheat a simulation model for wheat was initially developed and distributed with Decision Support System for Agro-technology Transfer (DSSAT) which simulates crop phenology and growth processes in response to different environmental and management factors. DSSAT_CERES_Wheat model have been applied under wide range of environmental conditions in response to different management practices and climate scenarios (Amirhajloo et al., 2023; Asseng et al., 2013, 2019; Attia et al., 2016; Chardon et al., 2012; Galmarini et al., 2024; Hussain et al., 2018; Salcedo, 2015). It simulates crop growth and development on daily time step in response to different factors such as cultivar, environment and management. Development rate in CERES-Wheat is governed by thermal time or growing degree days (GDD) approach computed on the daily time step from cardinal temperatures (maximum, minimum and optimum) using triangular or trapezoidal function. Specific number of GDD are required to shift from one growth stage to next. Daylength sensitivity affect the total number of leaves by altering the duration of the floral induction phase and thus floral initiation. Radiation se efficiency (RUE) approach (Light interception x RUE) has been used to modeled growth while development was affected by both temperature and daylength. Model converts daily intercepted photosynthetically active radiation (iPAR) into dry matter by using a crop specific RUE parameter. Light interception is calculated as function of LAI, plant population and row spacing. CERES-Wheat has individual plant growth modules that can simulate growth and yield for individual species. These modules can simulate phenology, daily growth and partitioning, plant nitrogen and carbon demands and senescence of plant material. Daily dry matter production by model is sensitive to water, nitrogen and temperature stress as well as atmospheric CO_2 concentration. Above ground biomass changes to carbohydrates on each day but carbohydrate which is not used for above ground biomass is allocated to roots. Kernel number per plant are computed during flowering based on canopy weight, average rate of carbohydrate accumulation during flowering, temperature, water and nitrogen stresses as well as cultivars genetic potential. Potential kernel growth rate (mg/(kernel d)) determines the daily grain growth rate based on a user defined cultivar input (Jones et al., 2003). Stem weight at anthesis is assumed to be proportional to grain number (Ritchie et al., 1998). Sets of species, ecotype and cultivars coefficients in the CERES-Wheat model define the phenology and crop growth in time domain. CERES-Wheat has been tested extensively against a range of studies from many different environments (Abbas et al., 2023; Ahmad et al., 2019; Ahmed et al., 2016; Andarzian et al., 2015; Attia et al., 2016; Ban et al., 2015; Basso et al., 2016; Dar et al., 2017; Jahan et al., 2018; Singh et al., 2015). However, CERES-Wheat has never been tested with source-sink manipulated data sets.

2.6. Model calibration

The procedure to use model includes calibration and evaluation. The data which were used for calibration comprises of environmental data, genotype features and field data from two sites i.e. Islamabad and URFK Chakwal during 2015–16. The model calibration was performed by considering data from optimum growth conditions i.e $N_3 = 100$ kg N ha^{-1} and 100 % RUE. The comparison of model simulations by DSSAT_CSM_wheat was carried out to assess the accuracy of crop simulation models. Different sets of crop species, cultivar and ecotype co-efficient files were used for model simulation which describes crop phenology and growth (Table 3). Estimation of genetic coefficients (GCs) was performed using Generalized Likelihood Uncertainty Estimation (GLUE) sub module of CSM-DSSAT and crop data. This method uses Bayesian estimation approach depending upon Monte Carlo sampling technique from prior distribution of genetic coefficients and Gaussian likelihood functions to define the preeminent genetic coefficients based on provided data for process estimation (Gauvain and Lee, 1994). Crop coefficients which were used for calibration were assessed by using observed data collected during wheat growing season of 2015–16 and it was checked through statistical indices i.e. values of root mean square error (RMSE) (Table 4). In genotype file of CERES-wheat (P1V, P1D, P5, and phyllochron interval) parameters controlled flowering and maturity dates (Andarzian et al., 2015) were adjusted for phenological simulations whereas to minimize the errors and discrepancies between observed and simulated values other files of ecotype (P1, P2, P3, G1 and G2) as recommended earlier (Ahmed et al., 2016) were also adjusted in this study.

Table 3
Calibrated wheat genetic coefficients for DSSAT-CERES-Wheat.

Crop file	Parameter	Default value	Calibrated Value
Species			
	TRGFW		
	Tbase[a]	0	4.5
	Topt1[b]	16	16
	Topt2[c]	35	33
	Tmax[d]	45	40
Ecotype			
	P1[e]	200	237
	P2[f]	200	300
	P3[g]	200	200
	P4[h]	200	200
	SLAS[i]	400	170
	PARUE[j]	2.7	4.5
	PARU2[k]	2.7	4.5
Genotype			
	PIV[l]	5	0
	PID[m]	75	85
	P5[n]	450	450
	G1[o]	30	13
	G2[p]	35	44
	G3[q]	1	3.2
	PHINT[r]	60	85

Where TRGFW: Temperature response, grain filling, dry weight (°C), [a]Base temperature (°C), [b]Optimum temperature 1, [c]Optimum temperature 2, [d]Maximum temperature, [e]Duration of phase end juvenile to terminal spikelet (PVTU),[f]Duration of phase terminal spikelet to end leaf growth (TU),[g]Duration of phase end leaf growth to end spike growth (TU),[h]Duration of phase end spike growth to end grain fill lag (TU),[i]Specific leaf area, standard first leaf (cm^2 g^{-1}), [j]Photosynthetic active radiation (PAR) conversion to dry matter (dm) ratio, before last leaf (g MJ^{-1}), [k]Photosynthetic active radiation (PAR) conversion to dry matter (dm) ratio, after last leaf (g MJ^{-1}), [l]Days, optimum vernalizing temperature, required for vernalization,[m]Photoperiod response (% reduction in rate/10 h drop in pp),[n]Grain filling (excluding lag) phase duration (oC.d),[o] Kernel number per unit canopy weight at anthesis (#/g),[p]Standard kernel size under optimum conditions (mg),[q]Standard, non-stressed mature tiller wt (incl grain) (g dwt), [r]Interval between successive leaf tip appearances (oC.d)

2.7. Model evaluation

To verify model performance we use validation, which is an important step and this process includes the comparison of the model predictions with the observed data. During growing seasons of 2015–16 and 2016–17 detailed field evidence were used to predict the impact of source sink partitioning in response of nitrogen fertilizer on wheat phenology (Days to anthesis and maturity), leaf area index, biomass production and grain yield at harvest was used to evaluate the model performance. The validation skills scores (R^2), d-index (Willmott, 1981) and RMSE were used to confirms the model robustness.

$$R^2 = 1 - \left[\frac{\sum (O_i - P_i)^2}{\sum (O_i - M_i)^2}\right]$$

Table 4
Calibration results of DSSAT-CERES-Wheat for crop phenology (Days to flowering and maturity), leaf area index (LAI), biomass (Kg ha^{-1}) and grain yield (Kg ha^{-1}) with RMSEs at Islamabad and Chakwal.

NARC-Islamabad				
Flowering (DAS)	Maturity (DAS)	LAI	Biomass (Kg ha^{-1})	Yield (Kg ha^{-1})
117 (RMSE=2.80 d)	149 (RMSE=2.53 d)	5.2 (RMSE = 0.57)	10696 (RMSE=379 kg ha^{-1})	3392 (RMSE=189 kg ha^{-1})
URF-Koont Chakwal				
Flowering (DAS)	Maturity (DAS)	LAI	Biomass (Kg ha^{-1})	Yield (Kg ha^{-1})
107 (RMSE=2.45 d)	141 (RMSE=2.05 d)	4.3 (RMSE = 0.80)	7666 (RMSE=179 kg ha^{-1})	1976 (RMSE=132 kg ha^{-1})

Where DAS: days after sowing, LAI: leaf area index, RMSE: root mean square error

$$d = 1 - \left[\frac{\sum_{i=1}^{n}(P_i - O_i)^2}{\sum_{i=1}^{n}(|P_i| + |O_i|)^2}\right]$$

$$\text{Root Mean Square Error} = \left[\sum_{i=1}^{n}\frac{(P_i - O_i)^2}{n}\right]^{1/2}$$

Where O, P and M represents observed, predicted and mean values for the treatments.

2.8. Water use efficiency

Biomass water use efficiency (BM_WUE) and grain water use efficiency (G_WUE) was calculated by using following formulas:

$$BM\_WUE = \frac{Dry\ matter\ at\ maturity(Kg\ ha^{-1})}{ET}$$

$$DM\_WUE = \frac{Grain\ yield(Kg\ ha^{-1})}{ET}$$

$$Where ET = \text{Evapotranspiration (mm)}$$

2.9. Statistical analysis

Four factors combinations including nitrogen fertilization (0, 50, 100, 150 and 200 kg N ha^{-1}), source-sink treatments (100 % RUE, 50 % RUE: shading and halving of spike), years (2015–16 and 2016–17) and locations (Islamabad and URFK Chakwal) were considered for data analysis followed by RCBD (Randomized complete block design) with three replications.

3. Results

3.1. Analysis of variance (ANOVA)

ANOVA table for four dependent variables (Locations, nitrogen levels, source-sink and years) with sources of variation (SOV), effect type, and degrees of freedom (df) have been shown in Table 5 with mean squares (MS) values for the fixed effects (FE) and random effects (RE). Since MS estimate the average variation associated with SOV and formulae to calculate MS is sum of square devided by degree of freedom thus MS plays a major role in estimating variance components in response to different treatments. MS values as shown in Table 5 clearly elaborates the variation due to different effects. MS values for days to anthesis and maturity shows that it remained significant for main effects as well as for some interactions. Similarly, for the leaf area index and biomass both main effect and interactions were significant. MS values for all other parameters have been shown in Table 5 with their

Table 5
ANOVA table for four dependent variables (Locations, nitrogen levels, source-sink and years) with sources of variation (SOV), effect type, and degrees of freedom (df). Mean squares (MS) values for the fixed effects (FE) and random effects (RE) are shown. Random effects used as error terms are shown in bold type.

			Mean Squares								
SOV	Effect†	df	DTA	DTM	LAI	Biomass	GY	HI	Soil N	CropN	GrainN
Replication (R)	**RE**	**2**	**1.25**	**0.27**	**6.403**	**19.59**	**1.5365**	**0.0003**	**637.9**	**3007.7**	**676.9**
Location (L)	FE	1	9.8*	2177.09**	190.76*	140.18*	11.3001*	0.000605*	32184.3*	49976.7*	6804.4*
Nitrogen levels (N)	FE	4	219.7**	253.34**	9.53*	18.412**	2.4365**	0.00194*	2044*	6108.3*	1022.5*
Source-sink (SS)	FE	2	240.2**	3943.47**	2.18*	285.264*	26.7485*	0.94756*	461.4*	535.4*	10321.2*
Years (Y)	FE	1	5^{NS}	0.09^{NS}	22.12*	6.365*	0.2205*	0.00365*	63.5*	170.7*	124.8*
L*N	FE	4	4.3^{NS}	23.99*	0.108*	0.423*	0.0463*	0.0002925*	286.2*	101.9*	30.8*
L*SS	FE	2	1.4^{NS}	149.57*	0.644*	3.317*	0.3224*	0.000665*	991.5*	608.6*	311.2*
L*Y	FE	1	5^{NS}	6.42*	10.804*	39.53*	8.9334*	0.0414*	928.9*	4756.6*	2209.9*
N*SS	FE	8	11.95*	15.23*	0.101*	0.597*	0.0728*	0.00048*	53.4*	23.6*	51.5*
N*Y	FE	4	5.8^{NS}	3.41*	0.287*	0.522*	0.0695*	0.00288*	12.6*	16.2^{NS}	30.3*
SS*Y	FE	2	1.93^{NS}	0.17^{NS}	0.228*	28.092*	0.8565*	0.01472*	550.7*	160.7*	655.7*
L*N*SS	FE	8	7.15*	11.83*	0.152*	0.207*	0.0103*	0.00024*	10.2*	19.3*	14.2*
L*N*Y	FE	4	2.03^{NS}	0.32^{NS}	0.06*	0.585*	0.0477*	0.0008425*	31.3*	5.6^{NS}	54.6*
L*SS*Y	FE	2	1.37^{NS}	2.21^{NS}	0.064*	3.18*	0.2404*	0.00979*	97.0*	135.6*	19.6*
N*SS*Y	FE	8	6.32^{NS}	1.97^{NS}	0.088*	0.252*	0.0059^{NS}	0.00019^{NS}	4.5^{NS}	42.7*	18*
L*N*SS*Y	FE	8	2.96^{NS}	1.09^{NS}	0.011*	0.4*	0.0034^{NS}	0.000535^{NS}	4.5^{NS}	20.2*	16.6*
Error	**RE**	**118**	**1.33475**	**0.93**	**0.005**	**0.024**	**0.0031**	**0.00017**	**1.7**	**5.6**	**1.2**

Where SOV: Source of variation, df: Degree of freedom, DTA: Days to anthesis, DTM: days to maturity, LAI: Leaf area index, GY: Grain yield, HI: Harvest index, Soil N: Soil nitrogen, CropN: Crop nitrogen, GrainN and Grain nitrogen.
*Significant at the 0.05 level.
** Significant at the 0.01 level.
†FE, fixed effect; RE, random effect.

significance levels. Mean squares values can be further used to calculate standard error of mean (SE) which has been used widely in the table of means as a measure of variation of means within a given population that indicates the precision of the mean. SE can also be sed further to estimate confidence interval of the mean.

3.2. Crop phenology

As shown in Fig. 4 crop phenology was reduced due to shading and spike halving treatment under varying nitrogen regimes at two different study sites. The CERES-Wheat model simulated this reduction with good accuracy showing close association with observed data. A greater number of days to anthesis (124) was simulated under N_{200} nitrogen application at Islamabad whereas the equivalent value for URFK Chakwal was (125). Among the source sink treatment, 6.4 and 6.6 percent reduction were found in simulated and observed values of shading over control. The smallest change in days to anthesis was found in different source-sink manipulation while the largest shift of simulated days to anthesis was 11.9 percent that was recorded in different nitrogen treatments. Fig. 4 shows a comprehensive impact of different source-sink and nitrogen treatments on days to anthesis. Similarly, predicted days to maturity have shown close association with observed data for different source sink partitioning and nitrogen regimes at Islamabad and Chakwal (Fig. 5). Maximum reduction of 6.5 % was predicted at Islamabad when crop was shaded at anthesis while spike halving treatments had increased days to maturity by 12 % as compared to control, whereas equivalent value for observed days to maturity were 9.7 and 1.28 %. Calculated validation skills scores i.e. R^2, RMSE and d-index were 0.89, 2.80 and 0.97 respectively for days to maturity at Islamabad. At URFK Chakwal simulated days to maturity have shown close association with observed data for different source sink partitioning and nitrogen regimes. Simulated days to maturity were reduced by 6.4 % during shading at anthesis whereas spike halving had increased days to maturity by 12.5 % over control, whereas equivalent values for observed days to maturity were 5.6 and 6.3 % for shading and spike halving. The values of validation skills scores at URFK Chakwal were R^2 (0.89), RMSE (2.65) and d-index (0.94).

3.3. Leaf area index

Simulated leaf area index (LAI) has shown close association with observed data for varying source sink partitioning and different nitrogen regimes (Fig. 6). At Islamabad maximum LAI were observed for spike halving and 100 % RUE at 150 kg N ha^{-1} while minimum was noted for 50 % RUE (shading). Meanwhile, the model predicted maximum and minimum LAI for spike halving and 50 % RUE treatments of source sink partitioning. On average calculated validation skills scores for LAI simulation for all treatments at Islamabad was R^2 (0.94), RMSE (0.51) and d-index (0.98). Furthermore, at URFK Chakwal highest (4.9) LAI was counted for spike halving whereas minimum (2.9) was recorded for 50 % RUE (Fig. 6). Among different nitrogen treatments maximum (4.9) and minimum (2.9) LAI was calculated for N_{150} and N_0 respectively. However, the model predicted LAI for N_{150} and N_0 was 4.8 and 3.1 respectively. The calculated validation skills scores for R^2, RMSE and d-index were 0.94, 0.38 and 0.92 respectively. Since our simulation results have shown close association between the observed and simulated values thus it confirms the model robustness.

3.4. Above-ground biomass (t ha^{-1})

Wheat biomass has shown close association with observed data for different source sink and nitrogen treatments under varying climatic conditions of Islamabad (Fig. 7) and URFK Chakwal (Fig. 8). Crop shading decreased the simulated above-ground biomass while spike halving had slightly decreased the biomass accumulation over control at Islamabad. The observed above ground biomass with shading was reduced by 43 % over control. The highest value of biomass accumulation (13.7 t ha^{-1}) was recorded for control at 100 kg N ha^{-1} followed by spike halving (11.5 t ha^{-1}) at 150 kg N ha^{-1} during 2015–16 at Islamabad while the lowest 7.0 t ha^{-1} was observed for 50 % RUE. However, the model estimated biomass for spike halving and 50 % RUE at 150 kg N ha^{-1} was 11.5 t ha^{-1} and 8.3 t ha^{-1} respectively. The 50 % reduction in RUE resulted to the 27 % decrease in biomass accumulation as compared to spike halving while 61 % in comparison with 100 % RUE at 150 kg N ha^{-1}. Similar trend was observed for all other N treatments and biomass accumulation was accurately simulated by CERES-Wheat. Among N treatments, maximum observed biomass (13.7 t ha^{-1}) was recorded for N_{100} while minimum (7.0 t ha^{-1}) was observed for N_0 during 2015–16 while biomass accumulation remained lower during 2016–17. Statistic indices values for evaluation of CERES-Wheat were R^2 (0.98), RMSE (370 kg ha^{-1}) and d-index (0.96) that have shown model potential to simulate above ground biomass. At URFK Chakwal the highest (9.8 t ha^{-1}) biomass was recorded for control under 100 kg N ha^{-1} during 2016–17 and it was well simulated by model. However, the lowest value was observed for crop shading (50 % RUE). The model efficiently simulated this effect but model overestimated the response of shading and have shown similar influence due to spike halving. Simulated results of nitrogen supply influenced the biomass accumulation and maximum biomass was simulated for 150 kg N ha^{-1}. Around 2 % higher biomass was simulated for 150 kg N ha^{-1} due to spike halving as compared to control while it was 32 % higher as compared to shading treatment. In general time series graphs show that model predicted biomass for source-sink partition with good accuracy (Figs. 7 and 8).

3.5. Grain yield (t ha^{-1})

Simulated grain yield has shown close association with observed data for varying source sink partitioning and different nitrogen regimes under different agro-climatic conditions of Islamabad and URFK Chakwal (Fig. 9). At Islamabad maximum grain yield (4.2 t ha^{-1}) was observed for 100 % RUE under 100 kg N ha^{-1} while minimum (1.7 t ha^{-1}) was recorded for spike halving for control N during 2015–16. Meanwhile, the model predicted maximum (4.1 t ha^{-1}) and minimum (1.7 t ha^{-1}) grain yield for 100 % RUE and spike halving treatments respectively. Shading (reduction of 50 % solar radiation) and spike halving decreased observed grain yield by 22 % and 46 % respectively as compared to control under 100 kg N ha^{-1}. The model simulated impact of different N levels and source sink partitioning on grain yield with good accuracy and calculated statistic indices values for R^2, RMSE and d-index was 0.97, 0.17 t ha^{-1} and 0.95 respectively. Similarly, model efficiently predicted grain yield similar to observed at URFK Chakwal. At URFK Chakwal maximum grain yield (2.8 t ha^{-1}) was observed for 100 % RUE under 150 kg N ha^{-1} whereas minimum value (1.2 t ha^{-1}) was recorded for spike halving 0 kg N ha^{-1} and they were close to the simulated values. Shading (reduction of 50 % solar radiation) and spike halving resulted to the decreased observed grain yield by 30 % and 46 % respectively under 150 kg N ha^{-1} as compared to control. However, percentage differences were higher under lower levels of N. Similar results were obtained for simulated grain yield for all source sink partioning and N treatments during both years. Furthermore, for N treatments maximum simulated and observed grain yield was obtained for N_{150} while minimum was noted for N_0 (Fig. 9). The model simulated grain yield with good accuracy and obtained validation skills scores at URFK Chakwal was R^2 (0.96), RMSE (0.2 t ha^{-1}) and d-index (0.93).

3.6. Harvest index

Simulated harvest index has shown close association with observed data for different source sink partitioning and varying nitrogen regimes under different agro-climatic conditions of Islamabad and URFK Chakwal (Fig. 10). At Islamabad higher harvest index (0.48) was

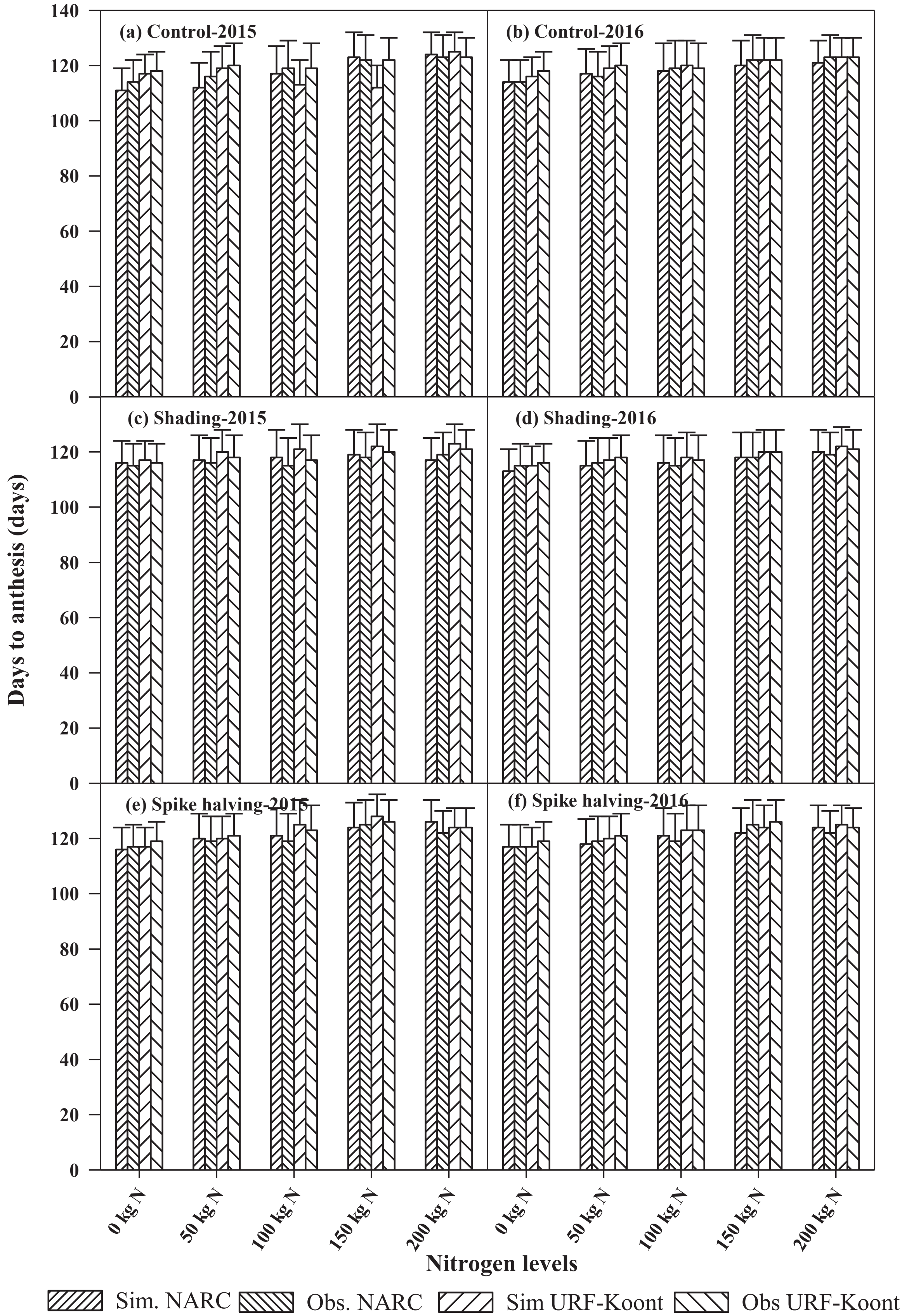

Fig. 4. Wheat days to anthesis (a) Control (100 % RUE) (b) shading (50 % RUE), and (c) spike halving under nitrogen fertilization at NARC Islamabad and URFK Chakwal.

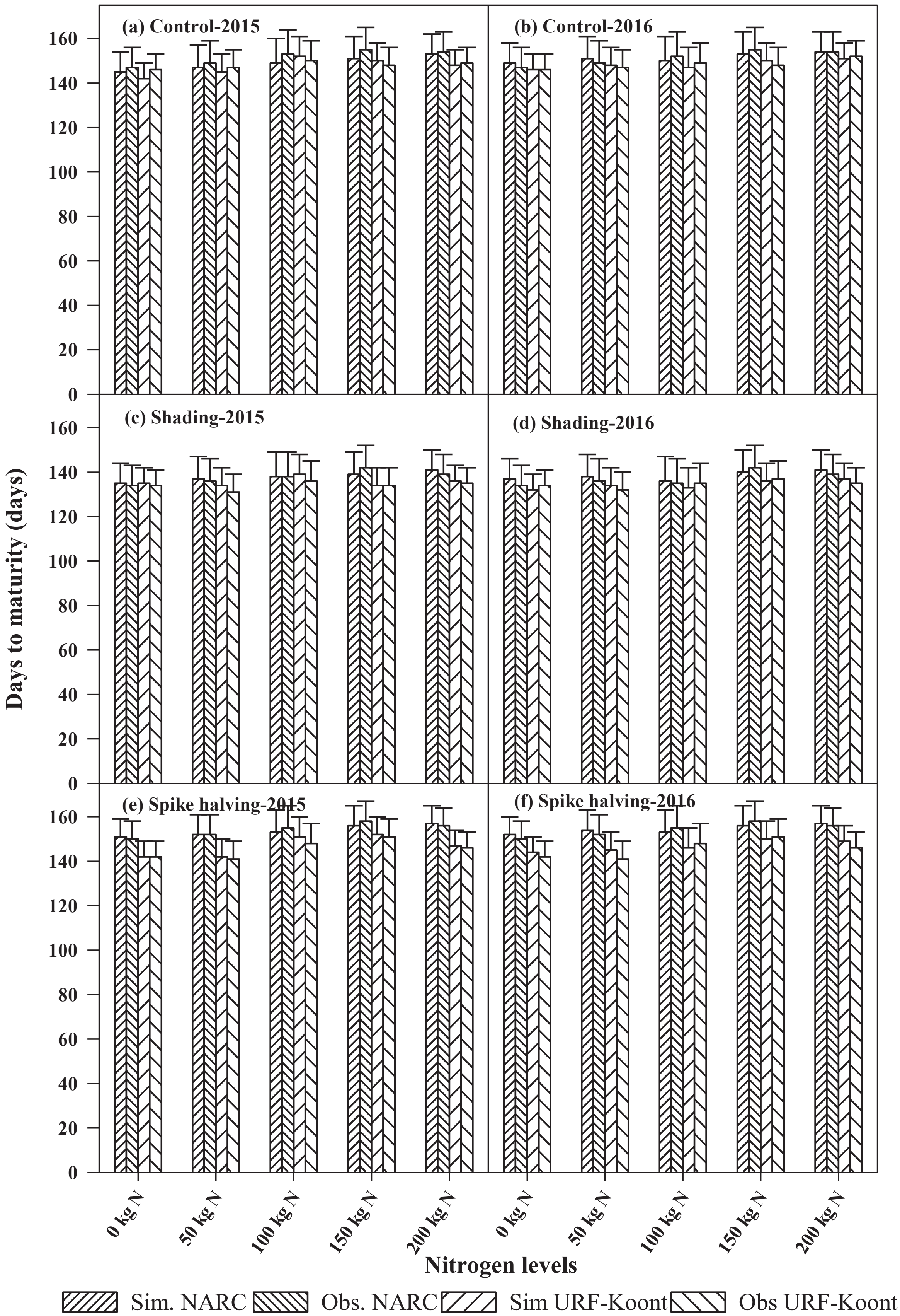

Fig. 5. Days to maturity (a) control, (b) shading (50 % RUE), and (c) spike halving in response to different nitrogen fertilization at NARC Islamabad and URFK Chakwal.

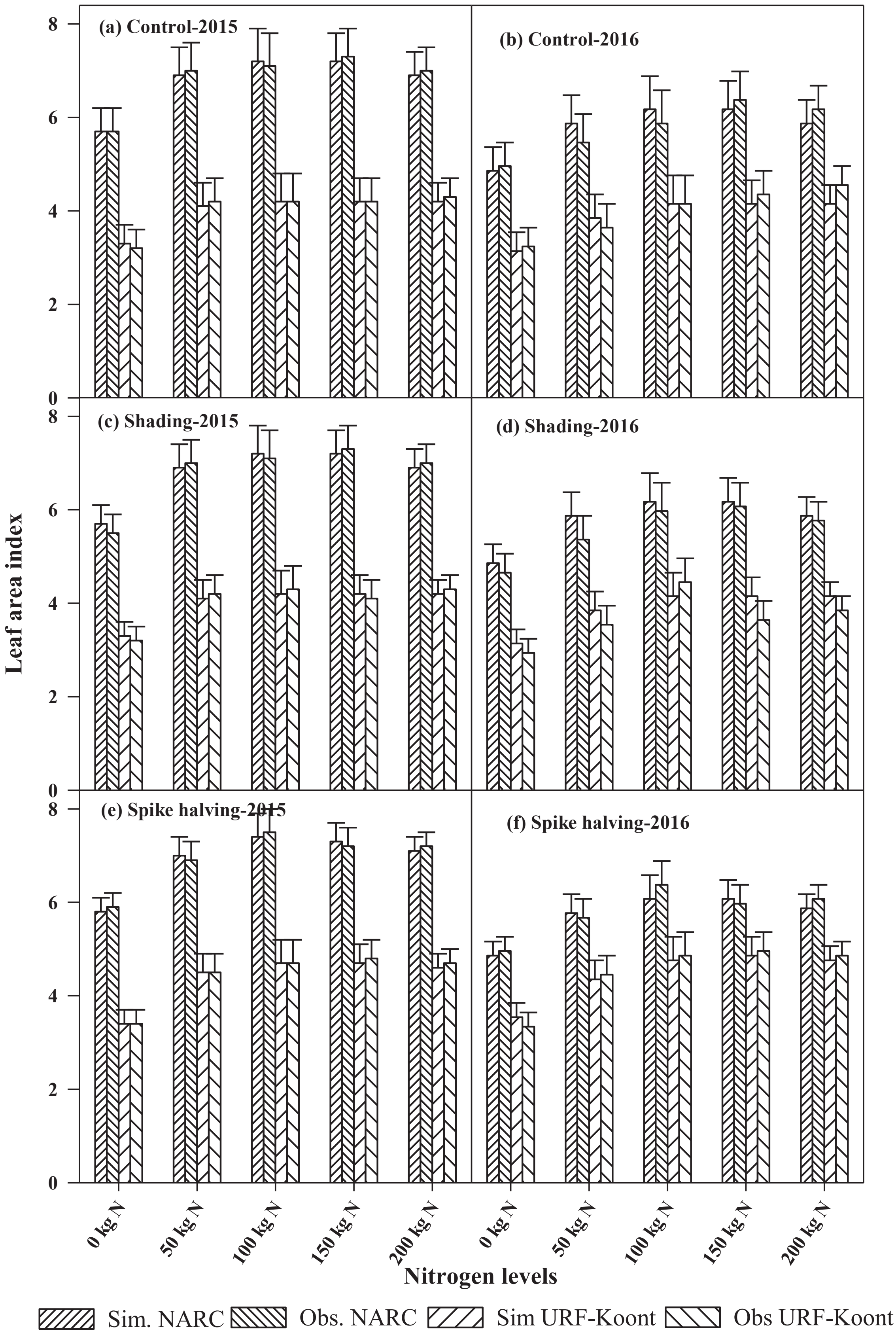

Fig. 6. Leaf area index (a) control, (b) shading (50 % RUE), and (c) spike halving in response to different nitrogen fertilization at NARC Islamabad and URFK Chakwal.

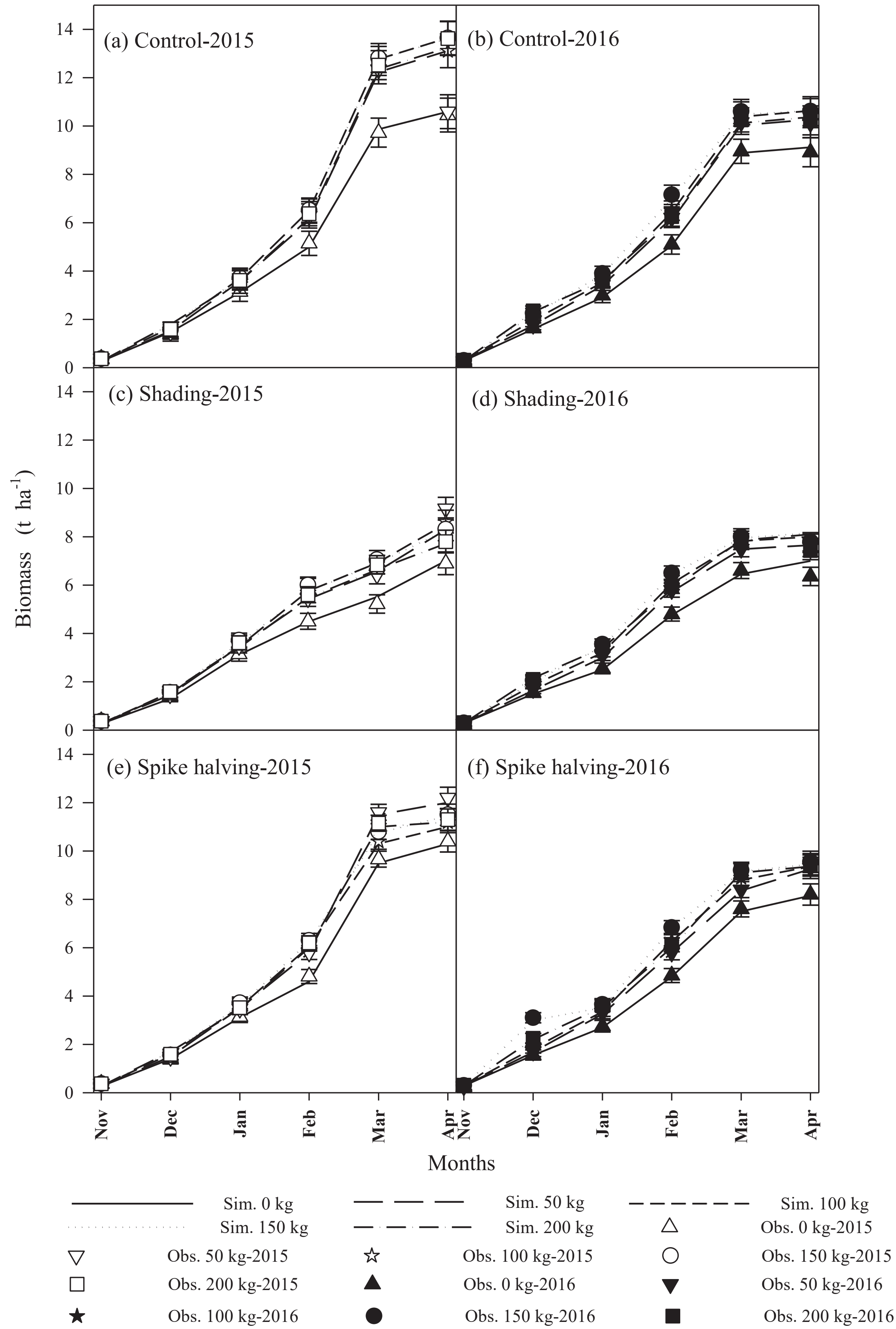

Fig. 7. Above ground biomass control (100 % RUE) (a, b), (b) shading (50 % RUE) (c,d), and (c) spike halving (e, f) in response to different nitrogen fertilization at NARC, Islamabad.

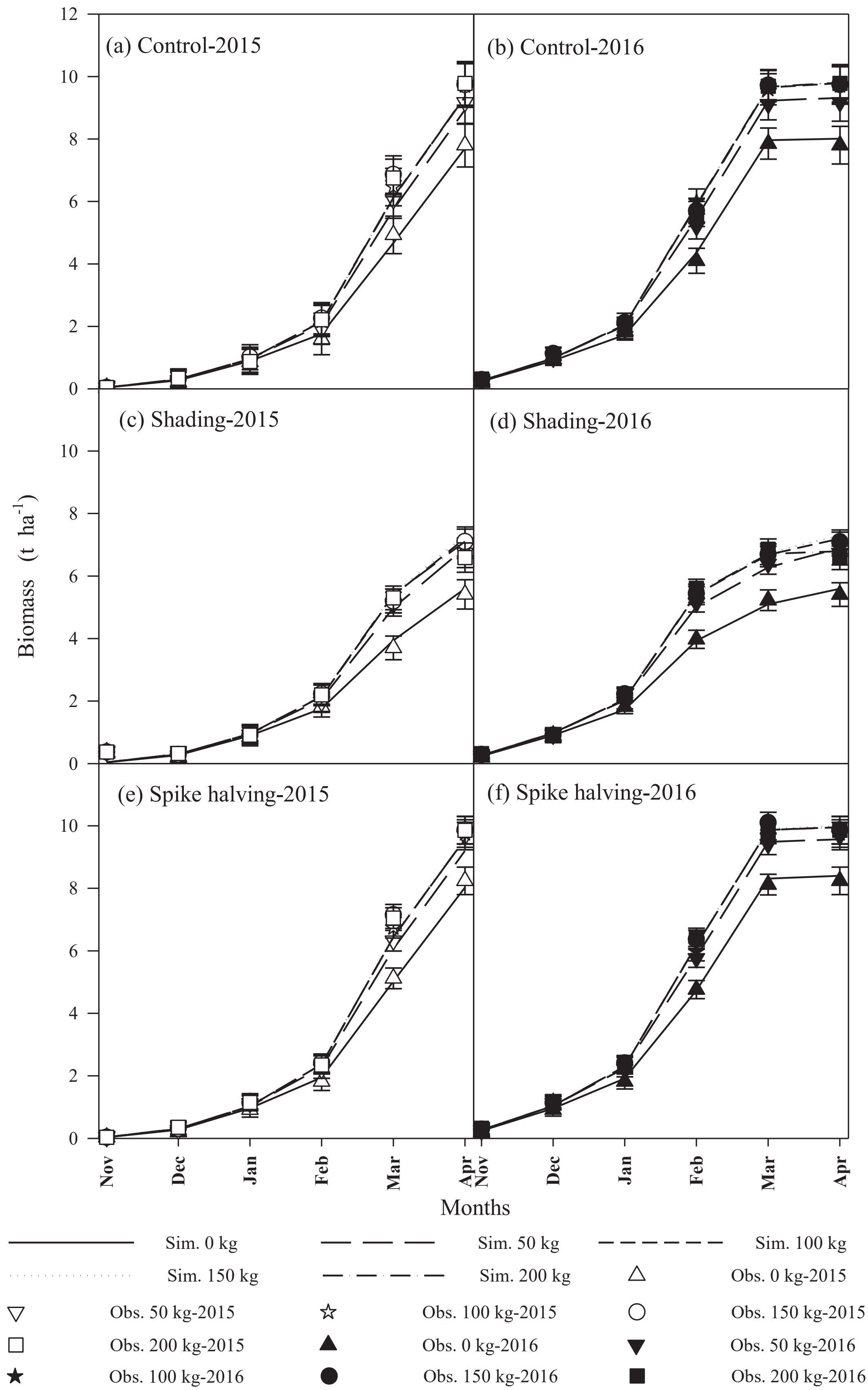

Fig. 8. Above ground biomass control (100 % RUE) (a, b), (b) shading (50 % RUE) (c,d), and (c) spike halving (e, f) in response to different nitrogen fertilization at URFK Chakwal.

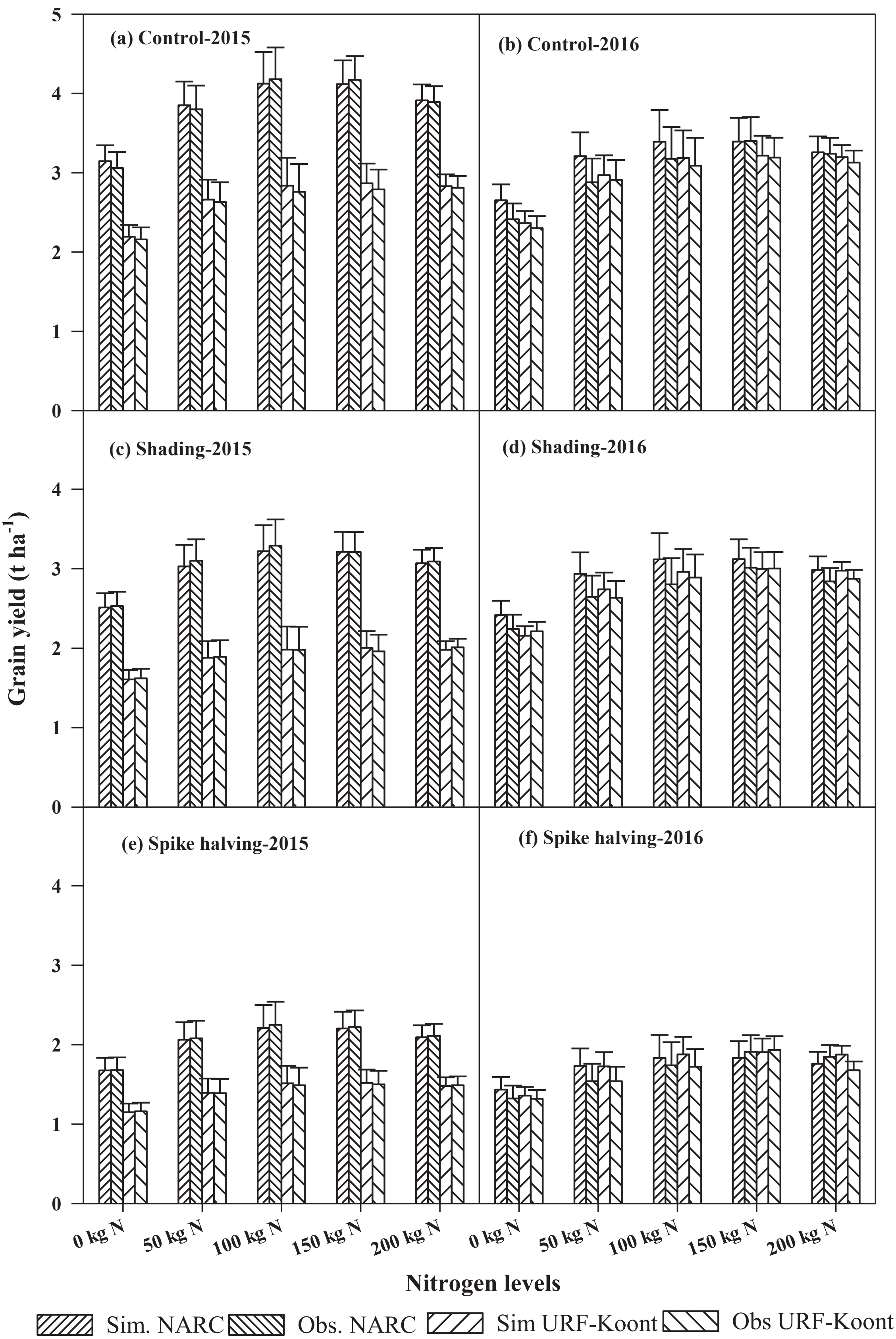

Fig. 9. Grain yield (a) control, (b) shading (50 % RUE), and (c) spike halving in response to different nitrogen fertilization at NARC Islamabad and URFK Chakwal.

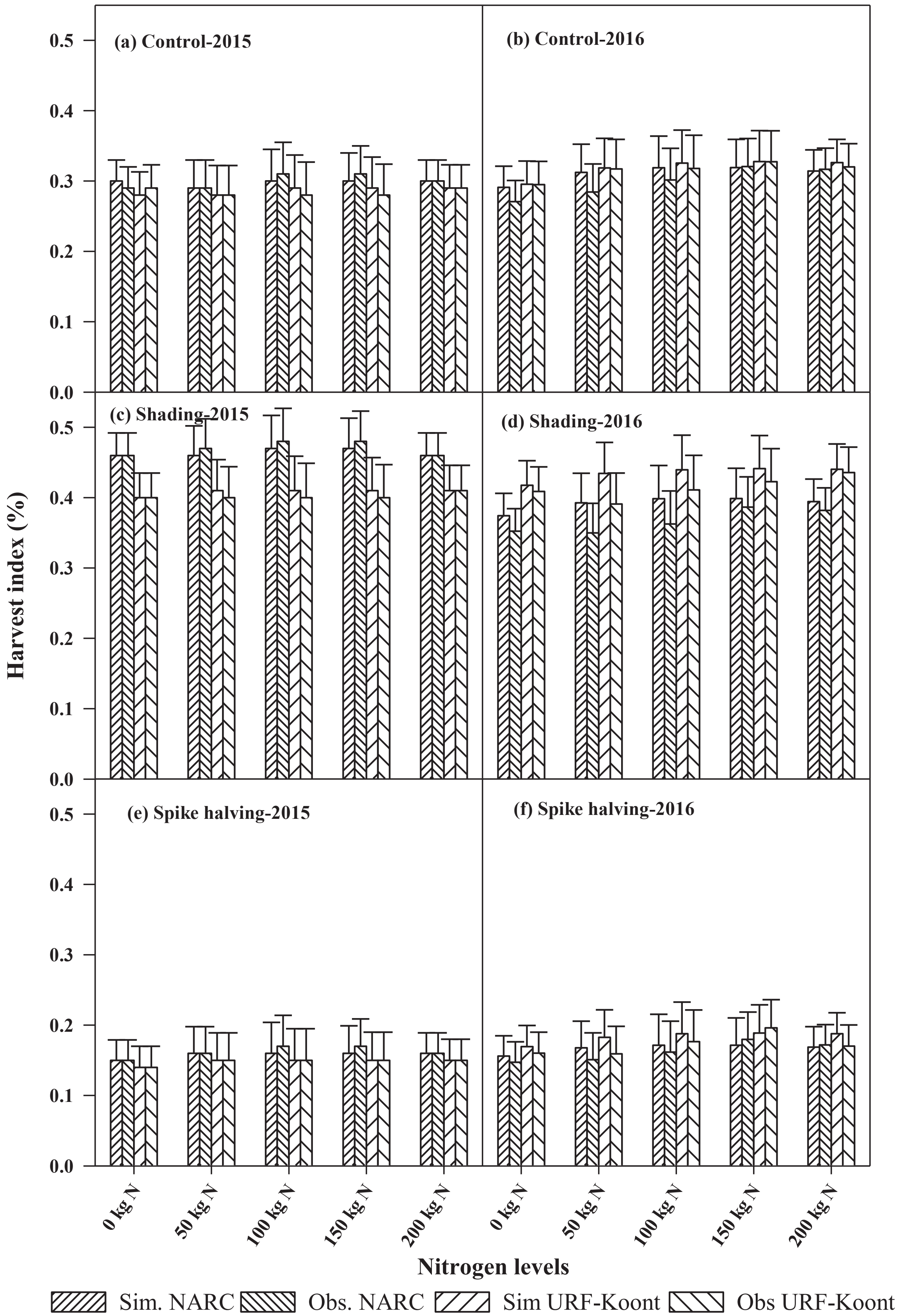

Fig. 10. Harvest index (a) control, (b) shading (50 % RUE), and (c) spike halving in response to different nitrogen fertilization at NARC Islamabad and URFK Chakwal.

observed for shading under N_{150} while minimum 0.15 was recorded for spike halving under N_0 during 2015–16. Meanwhile, the model predicted maximum (0.48) harvest index for spike halving treatment of source sink partitioning as compared to control (100 % RUE). The obtained values for the skill scores i.e. R^2, RMSE and d-index were 0.98, 0.05 and 0.93 respectively for Islamabad during both years. Similarly, at URFK Chakwal highest harvest index (0.41) was observed for 50 % RUE under N_{200} nitrogen application whereas minimum (0.14) was recorded for spike halving during 2015–16. A similar trend was observed for the second year. Furthermore, the model was able to simulate the effect of source sink partitioning under different N regimes on harvest index with good accuracy. At Islamabad maximum simulated harvest index (0.47) was recorded for 50 % RUE whereas minimum (0.15) was predicted for spike halving. Similarly, at URFK Chakwal maximum harvest index was simulated for 200 kg N ha^{-1} under shading while minimum value was simulated for spike halving under 0 kg N ha^{-1}. Calculated values for R^2, RMSE and d-index were 0.98, 0.04 and 0.94 respectively at URFK Chakwal which shows the robustness of model to simulate harvest index.

3.7. Nitrogen dynamics (Soil mineral N, Crop and Grain N)

Nitrogen dynamics (Soil mineral N, Crop and Grain N) simulations under five different nitrogen and three source-sink treatments have shown close associations with field observed data (Figs. 11–13). Highest soil mineral N was simulated for 50 % RUE under N_{150} at URFK Chakwal and it was close to the observed value. However, lowest values were simulated for spike halving (Fig. 11) under control treatment of soil mineral N at Islamabad during 2015–16. A similar trend was simulated at both sites during 2016–17 for soil mineral N but it remained slightly higher than soil mineral N values during 2015–16. Validation skill scores obtained for the shading treatments under all N treatments at URFK Chakwal was R^2=0.97, RMSE=3.4 kg N ha^{-1} and d-index = 0.97. Furthermore, the model simulated crop N with good accuracy as shown in Fig. 12. During 2015–16 at Islamabad highest crop N was observed for control under 100 Kg N ha^{-1} while it remained lowest for shading under 0 kg N ha^{-1}. There was close association between observed and simulated values of crop N during 2015–16 with skill scores values of R^2 = 0.99, RMSE = 2.6 kg N ha^{-1} and d-index of 0.99. Similar trend was observed and simulated during 2016–17 but with lower crop N as compared to 2015–16. At URF-Koont highest N uptake was observed for control under 200 kg N ha^{-1} while lowest value was noted for shading under 0 kg N ha^{-1} and these were well simulated by CERES-Wheat during both years (Fig. 12). Similar results were obtained for Grain N (Fig. 13).

3.8. Water use efficiency

Variable biomass water use efficiency (BM_WUE) (kg ha^{-1} mm^{-1}) was observed in response to years, locations, nitrogen levels and source-sink treatments (Table 6). At Islamabad during 2015–16, highest BM_WUE (34.1 kg ha^{-1} mm^{-1}) was calculated for the spike halving treatments at 50 kg N ha^{-1} while lowest (14.7 kg ha^{-1} mm^{-1}) was obtained for shading (50 % RUE) at 0 kg N ha^{-1}. Similarly, at URFK Chakwal during 2015–16 maximum BM_WUE (29.6 kg ha^{-1} mm^{-1}) was calculated for spike halving at 50 kg N ha^{-1} while minimum BM_WUE (14.5 kg ha^{-1} mm^{-1}) was obtained for shading (50 % RUE) at 0 kg N ha^{-1}. Similar trend was observed for BM_WUE during 2016–17. However, in second year BM_WUE were considerably lower than the BM_WUE during 2015–16.

Grain water use efficiency (G_WUE) (kg ha^{-1} mm^{-1}) values in response to years, locations, nitrogen levels and source-sink treatments have been shown in Table 7. The highest G_WUE at Islamabad during 2015–16 was 10.3 kg ha^{-1} mm^{-1} for the control (100 % RUE) under 150 kg N ha^{-1} while lowest was 4.4 kg ha^{-1} mm^{-1} for the spike halving under 0 kg N ha^{-1}. Similarly, maximum G_WUE (8.5 kg ha^{-1} mm^{-1}) at Chakwal during 2015–16 was calculated for the control (100 % RUE) under 150 kg N ha^{-1} which was at par with other N treatments in 100 % RUE as well as in 50 % RUE. However, minimum G_WUE (3.7 kg ha^{-1} mm^{-1}) at URFK Chakwal during first year was observed for the spike halving under 0 kg N ha^{-1}. During 2016–17, trend of G_WUE at Islamabad was similar but at URFK Chakwal calculated G_WUE was highest as compared to 2015–16. Results shows that during 2016–17 at URFK Chakwal the highest G_WUE was 12.5 kg ha^{-1} mm^{-1} for shading (50 % RUE) under 150 kg N ha^{-1}

4. Discussions

Source sink modification under different N levels resulted to the significant changes in the recorded crop parameters which was at par with the findings of Lv et al. (2020) who reported that grain yield is due to synergistic interaction between source activity and sink capacity. Similarly, sink strength has direct relationship with leaf area as it determines the crop capacity to produce photosynthate during vegetative growth. In our studies ANOVA (Table 5) have shown that LAI have been significantly improved due to N applications. The interactive effect of N on LAI with all other dependent variables were significant. Furthermore, Fu et al. (2011) reported that strong source with good reserves is needed for good grain filling while high sink capacity promotes reserve remobilization from the source to sink. In the present study, the values of LAI were maximum for 100 % RUE at 150 kg N ha^{-1} while minimum was noted for 50 % RUE (shading) under 150 kg N ha^{-1} which shows that N and source sink have strong impact in the determination of LAI activity (Fig. 6).

Our results were not at par with the findings of Heİdari (2023) who studied the effect of nitrogen rate (Source) and spikelet removal (Sink i.e. no spikelet removal and ½ spikelet removal) on seed yield and germination traits of wheat and reported no change in seed yield and seed weight due to source and sink manipulation. Furthermore, he concluded that wheat variety used in this study was more sink-limited than source-limited. Similar to our work impact of different agronomic practices on the regulation of source-sink to increase water use and grain yield of wheat crop was studied by Fang et al. (2022). They concluded that leaf area and dry matter plays a decisive role in increasing crop yield and recommended that 180 kg N ha^{-1} with other agronomic measures could balance the source-sink in order to have higher yield and WUE. Synthesis of dry matter, LAI and establishment of yield components as highlighted by Asseng et al. (2017) have strong association with soil conditions such as water and nutrients as seen in our work where soil mineral N, crop N and grain N was significantly changed in response to dependent variables (Table 5, Figs. 11,12 and 13). However, lower nutrient absorption was observed at URFK Chakwal mainly because of water shortage (Wang et al., 2010). Since N application increases crop LAI, dry matter, grain yield and water productivity thus a metanalysis was conducted by Wang et al. (2023) to recommend optimum N management. They suggested that 100–200 kg N ha^{-1} is good to maximize crop yield and WUE. Bongiovani et al. (2024) studied the effect of lower N and reduced rainfall on wheat yield which is similar to our work at URFK Chakwal (low rainfall site). They concluded that cultivation without N fertilizer inputs might be possible over a few years if soil N_{min} is greater than 50 kg ha^{-1} and it will be only for those wheat genotypes which has higher grain numbers per m^2 and water-soluble carbohydrates. Gui et al. (2024) studied the relationship of source sink and water deficit on dry land wheat. They reported that drought stress resulted to reduced dry matter and grain yield as we reported for the low rainfall site i.e. URFK Chakwal. However, they reported that high ploidy wheat exhibited sustainable grain yield due to its buffering capacity between source supply and sink demand.

Accurate prediction of crop phenology is important to do crop management effectively (Azmat et al., 2021; Fatima et al., 2020; Gao et al., 2020; Menzel et al., 2020). Since crop phenology is mainly driven by climatic variables like temperature and solar radiation thus modification in source-sink balance resulted to changes in crop phenology

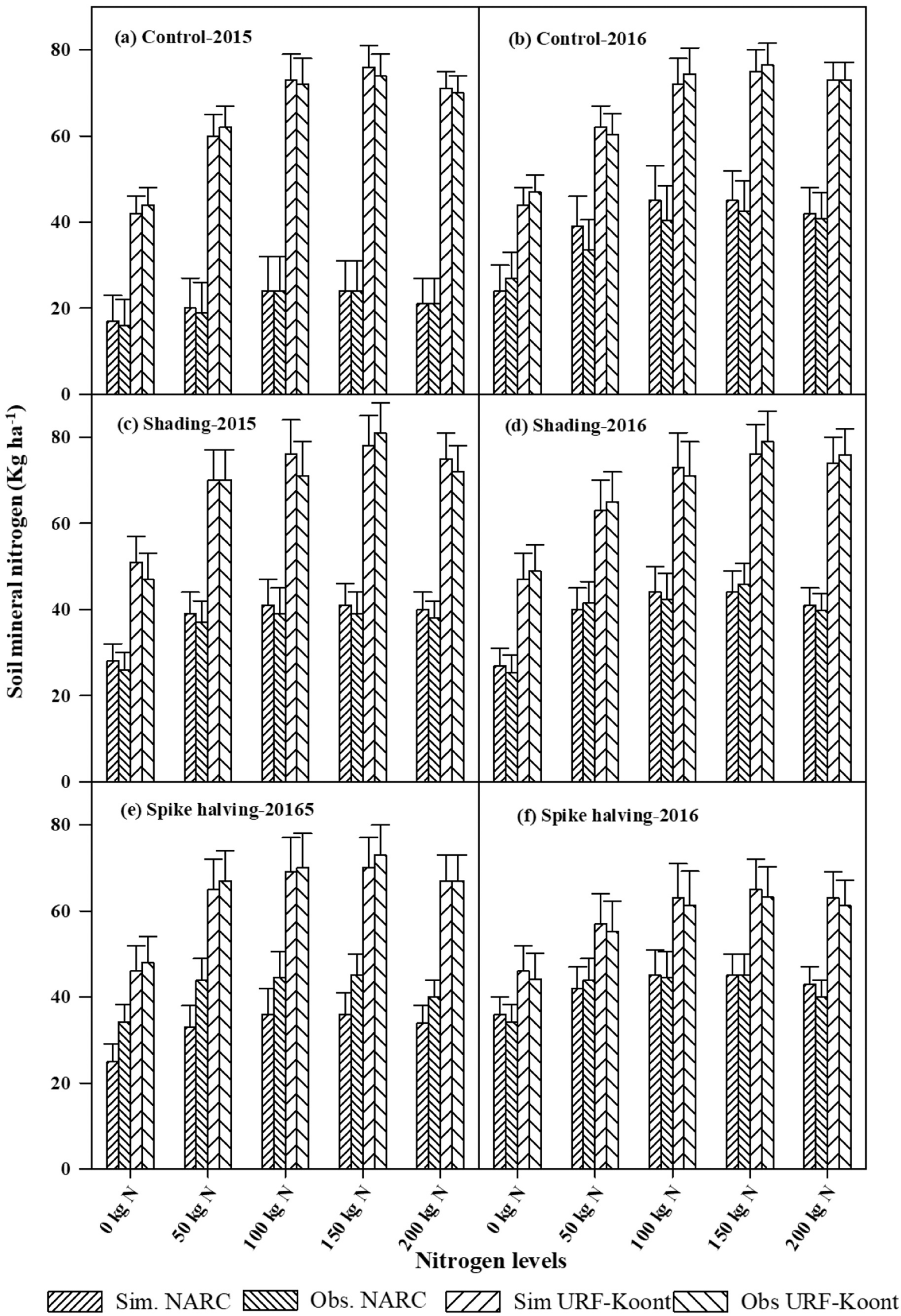

Fig. 11. Soil mineral nitrogen (kg ha^{-1}) (a) control, (b) shading (50 % RUE), and (c) spike halving in response to different nitrogen fertilization at NARC Islamabad and URFK Chakwal.

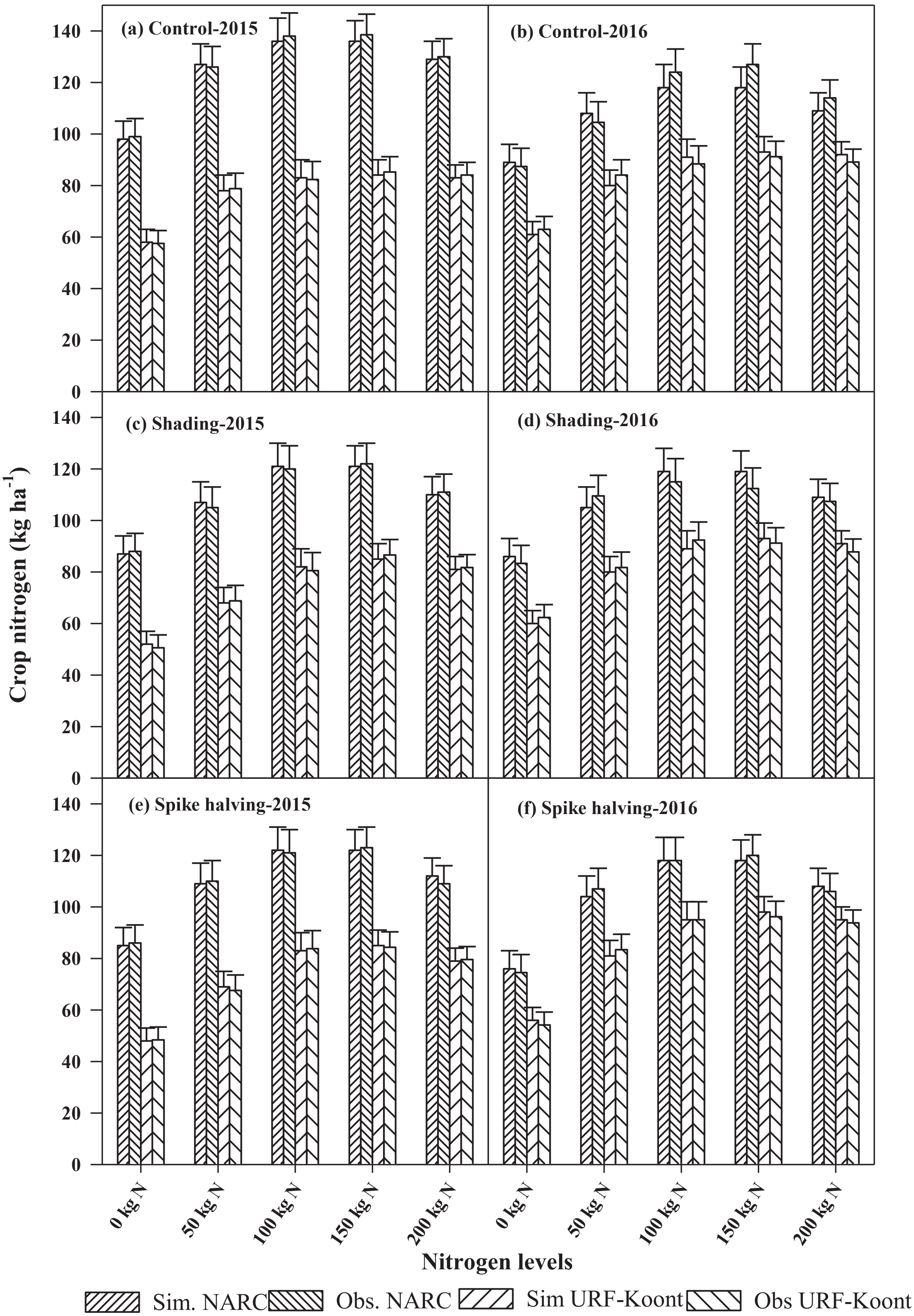

Fig. 12. Crop nitrogen (kg ha^{-1}) (a) control, (b) shading (50 % RUE), and (c) spike halving in response to different nitrogen fertilization at NARC Islamabad and URFK Chakwal.

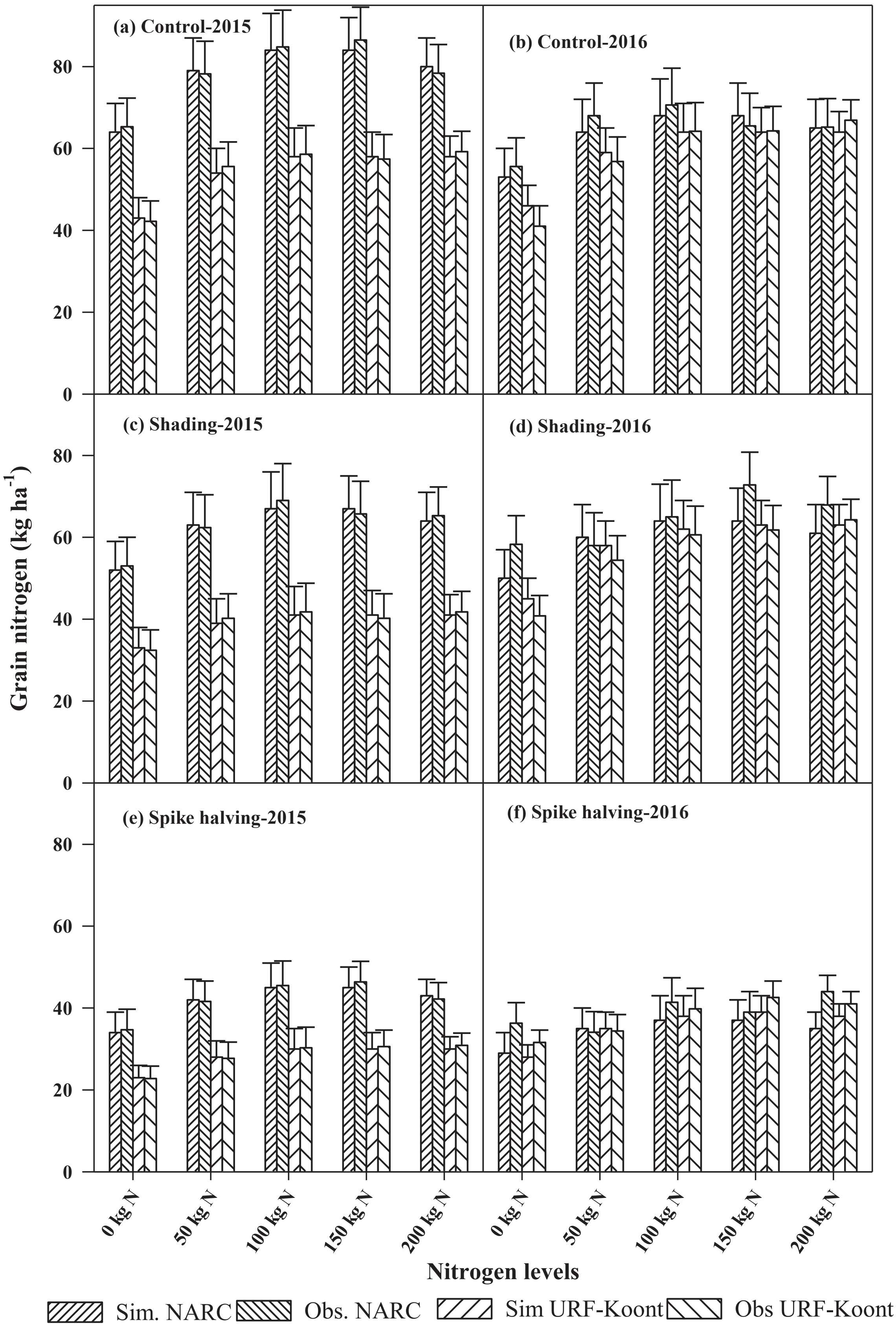

Fig. 13. Grain nitrogen (a) control, (b) shading (50 % RUE), and (c) spike halving in response to different nitrogen fertilization at NARC Islamabad and URFK Chakwal.

Table 6
The effect of years, locations, nitrogen levels and source-sink treatments on dry matter yield (kg ha^{-1}), evapotranspiration (ET) (mm) and biomass water use efficiency (BM_WUE) (kg ha^{-1}mm^{-1}).

Years		2015–16						2016–17					
Source-sink\Locations		Islamabad			Chakwal			Islamabad			Chakwal		
Control	Nitrogen levels	Yield	ET	BM_WUE	Yield	ET	BM_WUE	Yield	ET	BM_WUE	Yield	ET	BM_WUE
(100 % RUE)	N_0	10450^{f}	397.2	26.3^{f}	7743^{d}	321.7	24.1^{d}	8910^{d}	397.0	22.4^{e}	7800^{e}	282.1	27.7^{f}
	N_{50}	10590^{f}	401.2	26.4^{f}	9097^{c}	325.0	28.0^{b}	10120^{c}	399.6	25.3^{b}	9170^{c}	285.3	32.1^{d}
	N_{100}	13110^{a}	412.4	31.8^{d}	9539^{b}	334.0	28.6^{b}	10530^{b}	406.2	25.9^{b}	9710^{b}	294.6	33.0^{c}
	N_{150}	13640^{a}	404.5	33.7^{b}	9565^{b}	327.6	29.2^{b}	10610^{a}	402.8	26.3^{ab}	9740^{a}	287.7	33.9^{b}
	N_{200}	13620^{a}	408.6	33.3^{b}	9390^{b}	331.0	28.4^{b}	10230^{c}	418.9	24.4^{c}	9780^{a}	287.1	34.1^{b}
Shading	N_0	5220^{j}	355	14.7^{i}	4160^{f}	287.6	14.5^{f}	6360^{g}	348.5	18.2^{f}	5410^{h}	253.9	21.3^{h}
(50 % RUE)	N_{50}	6430^{i}	344.3	18.7^{h}	4740^{e}	278.9	17.0^{e}	7560^{f}	340.4	22.2^{e}	6740^{g}	245.6	27.4^{f}
	N_{100}	6850^{h}	360.7	19.0^{h}	4940^{e}	292.2	16.9^{e}	7730^{e}	352.9	21.9^{e}	7030^{f}	258.4	27.2^{f}
	N_{150}	7050^{g}	344.3	20.5^{g}	4880^{e}	278.9	17.5^{e}	7790^{e}	361.7	21.5^{e}	7100^{f}	239.4	29.7^{e}
	N_{200}	6840^{h}	371.8	18.4^{h}	4860^{e}	301.2	16.1^{e}	7430^{f}	352.9	21.1^{e}	6590^{g}	269.5	24.5^{g}
Spike Halving	N_0	11010^{e}	383.1	28.7^{e}	7810^{d}	310.3	25.2^{c}	8990^{d}	383.1	23.5^{d}	8239^{d}	272.0	30.3^{e}
	N_{50}	12940^{d}	379.8	34.1^{a}	9100^{c}	307.6	29.6^{a}	10200^{c}	378.8	26.9^{a}	9672^{b}	269.9	35.8^{a}
	N_{100}	13470^{b}	404.5	33.3^{b}	9510^{b}	327.6	29.0^{b}	10760^{a}	402.8	26.7^{ab}	9752^{a}	287.7	33.9^{b}
	N_{150}	13590^{a}	415.8	32.7^{c}	9810^{a}	336.8	29.1^{b}	10630^{a}	414.5	25.6^{b}	9865^{a}	295.6	33.4^{c}
	N_{200}	13240^{c}	401.2	33.0^{bc}	9860^{a}	325.0	30.3a	10740a	397.0	27.1^{a}	9855^{a}	286.1	34.4^{b}

Values followed by different uppercase letters indicate significance at $P < 0.05$.

Table 7
The effect of years, locations, nitrogen levels and source-sink treatments on yield (kg ha^{-1}), evapotranspiration (ET) (mm) and grain water use efficiency (G_WUE) (kg ha^{-1} mm^{-1}).

Years		2015–16						2016–17					
Source-sink\Locations		Islamabad			Chakwal			Islamabad			Chakwal		
Control (100 % RUE)	Nitrogen levels	Yield	ET	G_WUE	Yield	ET	G_WUE	Yield	ET	G_WUE	Yield	ET	G_WUE
	N_0	3060^{f}	397	7.7^{b}	2160^{c}	322	6.7^{a}	2411e	397	6.1^{b}	2301^{e}	282	8.2^{c}
	N_{50}	3800^{c}	401	9.5^{a}	2630^{b}	325	8.1^{a}	2879c	400	7.2^{ab}	2910^{cd}	285	10.2^{b}
	N_{100}	4180^{a}	412	10.1^{a}	2760^{a}	334	8.3^{a}	3175a	406	7.8^{a}	3089^{b}	294	10.5^{b}
	N_{150}	4170^{a}	405	10.3^{a}	2790^{a}	327	8.5^{a}	3401a	403	8.4^{a}	3191^{a}	288	11.1^{a}
	N_{200}	3890^{b}	409	9.5^{a}	2810^{a}	331	8.5^{a}	3239a	420	7.7^{a}	3128^{a}	287	10.9^{b}
Shading (50 % RUE)	N_0	2530^{g}	355	7.1^{bc}	1620^{f}	288	5.6^{b}	2240 f	349	6.4^{b}	2212^{e}	254	8.7^{c}
	N_{50}	3100^{f}	344	9.0^{ab}	1890^{e}	279	6.8^{a}	2644d	340	7.8^{a}	2634^{e}	246	10.7^{b}
	N_{100}	3290^{d}	361	9.1^{ab}	1980^{d}	292	6.8^{a}	2802c	353	7.9^{a}	2889^{cd}	258	11.2^{a}
	N_{150}	3210^{e}	344	9.3^{ab}	1960^{d}	279	7.0^{a}	3013b	362	8.3^{a}	3001^{bc}	239	12.5^{a}
	N_{200}	3090^{f}	372	8.3^{b}	2010^{d}	301	6.7^{a}	2839c	353	8.0^{a}	2873^{d}	269	10.7^{b}
Spike Halving	N_0	1680^{j}	383	4.4^{c}	1160^{i}	310	3.7^{b}	1324j	383	3.5^{d}	1320^{i}	272	4.9^{e}
	N_{50}	2080^{i}	380	5.5^{c}	1390^{h}	308	4.5^{b}	1540i	379	4.1^{c}	1541^{h}	270	5.7^{d}
	N_{100}	2250^{h}	404	5.5^{c}	1490^{g}	328	4.5^{b}	1739 h	403	4.3^{c}	1723^{g}	288	6.0^{d}
	N_{150}	2220^{h}	415	5.3^{c}	1500^{g}	337	4.5^{b}	1910 g	415	4.6^{c}	1935^{f}	296	6.5^{d}
	N_{200}	2110^{i}	401	5.2^{c}	1490^{g}	325	4.6^{b}	1845 g	397	4.6^{c}	1678^{g}	286	5.9^{d}

Values followed by different uppercase letters indicate significance at $P < 0.05$.

(Ahmed et al., 2016; Anwar et al., 2015; Aslam et al., 2017; Hussain et al., 2018; Monzon et al., 2007; Rezaei et al., 2015; Wallach et al., 2019; Wang et al., 2015; Wang and Engel, 1998; Yan and Wallace, 1998; Zeng et al., 2011). In our findings, CERES-wheat outcomes adequately predicted phenology of wheat crop (days to anthesis and maturity) under different sets of treatments and it was at par with earlier work (Ahmed et al., 2016; Hafiza et al., 2022; Ishaque et al., 2023; Wallach et al., 2023). Hence accurate prediction of crop phenology through crop models could assist crop managers, agronomist and breeders to do crop management operations accurately as well as to design future crop ideotypes under different sets of managements and environments (Kephe et al., 2021; Potgieter et al., 2021; Yu et al., 2023).

Crop growth and development are associated to photosynthates formation and radiation use efficiency (Lázaro et al., 2010). Photosynthesis is engine of crop productivity. Hence modifications in the source-sink balance of plants can result in changes in the leaf area as visible in our results and thus photosynthesis, dry matter and yield. This could be because of higher interception of light due to expansion of leaf that resulted to the larger leaf area (Cai et al., 2021; Mahakosee et al., 2022). Source-sink are the two factors which effect above-ground biomass of wheat. Strong correlation was found in biomass growth and intercepted photosynthetic active radiation in the work of Lázaro et al. (2010). In our field experiment above-ground biomass was reduced (27.8 %) by source reduction (shading) whereas sink reduction increased (2.2 %) above-ground biomass. Increased above-ground biomass due to sink reduction might be due to decrease in sink capacity as a result the assimilate partitioning moved towards other parts of the plant. Our results was supported by Sinclair and Jamieson (2006) who described that availability of adequate resources (source supply) is the key determinant to biomass accumulation. Higher wheat biomass was due to variability in seasonal weather as Islamabad brought forth favorable environment with higher rainfall and temperature as compared to URFK Chakwal. Furthermore, reduction in biomass yield may be due to various reasons but according to current research findings the most limiting factor was decrease in source and sink activity. It has been documented in earlier work that biomass accumulation played more important role in final yield (Li et al., 2023). Biomass simulation at maturity adequately confirms the ability of CERES-wheat model to predict biomass at harvest in rainfed conditions. Wheat production is source limited up to anthesis while source-sink co-limited during grain filling stage reported by Serrago et al. (2013). Source limitation is highly affected by source size and source activity. Our results supported the outcomes of Arora et al. (2007) in which they reported that CERES-wheat can simulate crop biomass.

Results of Álvaro et al. (2008) are in line to our findings in which they concluded that by reducing the source capacity through shading had negative effect on grain yield which could be due to less interception of solar radiation and lower photosynthetic rate. Similarly, Xiao-li et al. (2022) reported that grain potential is more source limited during grain filling but source-sink balance could be changed due to N limitations, water availability and climatic variations as depicted in our work. Similarly effect of source-sink manipulation on crop growth parameters can be simulated by using process based models like DSSAT. Asseng et al. (2016) reported that models have the ability to simulate wheat phenology closer to observed values. Our findings validated the outcomes of Asseng and Van Herwaarden (2003) who reported that when source is reduced grain yield relied on reserved carbohydrates whereas sink reduction (spike halving) directly decreased number of kernel per unit area. Previously Miralles and Slafer (2007b) and Reynolds et al. (2007) reported that compared to source, sink limitation contributed more negatively towards final grain yield of wheat as seen in our results of spike halving. However, increase in nitrogen application had meaningful impact on sink parameters of wheat as seen in our findings. Warraich et al. (2002) reported increase in grain yield of wheat crop due to application of nitrogen. Furthermore, they concluded that sink parameters may be regulated by increasing availability of nitrogen. The results of Fan and Li (2001) were in line with our results where they concluded that deficient nitrogen reduces grain yield. Additionally, they reported that by strengthening the sink capacity wheat yield could be improved. Simulated grain yield is directly related to crop canopy radiation interception, radiation use efficiency, sink activity/capacity and harvest index (Asseng et al., 2016). Shading during grain filling decreases interception of solar radiation and photosynthetic activity and explore the functional dynamics of source-sink interactions and effect on yield related attributes of wheat (Asseng et al., 2016). Our results revealed that source reduction resulted to 8.1 % decrease in grain yield while sink limitation resulted to the 46 % reduction in grain yield. Simulation outcomes of CERES-wheat model revealed that spike halving could reduce kernel number per unit area while shading reduces grain weight of wheat which might affect wheat yield. Our findings are consistent with outcomes of Borrás et al. (2004b) who reported that grain yield of wheat depends upon the timing of source and sink limitation during different growth stages. Simulation results of our experiment confirm the efficiency and application of crop models in physiological activities (Enders et al., 2023; Galmarini et al., 2024; Pasley et al., 2023).

In rainfed agriculture WUE is one of the important criteria to check dry matter and grain yield productivity per drop of water. Biomass WUE can be determined by dry matter yield per unit of water consumed while grain WUE can be calculated by grain yield per unit of water consumption and it has been reported that WUE is linearly correlated with yield (Ram et al., 2013). Higher BM_WUE (kg $ha^{-1}mm^{-1}$) at Islamabad during 2015–16 in spike halving treatment under 50 kg N ha^{-1} could be due to effective conversion of water into photosynthate as compared to URFK Chakwal. However, during 2016–17 higher BM_WUE was calculated for URFK Chakwal that could be due to low ET and effective conversion of available water to biomass as compared to Islamabad where higher ET resulted to reduced WUE (Fang et al., 2024). Similar trend in case of G_WUE could be due to effective ET and its positive relationship with nitrogen levels and source-sink treatments. Generally it has been reported that higher WUE can be achieved by managing soil water and adjusting crop sowing time so that critical growth stages matches with the prevailing spell of rainfall (Abbas et al., 2023; Ahmed et al., 2014; Hafiza et al., 2022; Ishaque et al., 2023; Xu et al., 2016). Furthermore, deficit irrigation strategy should be used as it can improve yield and WUE by regulating source-sink relationship under water deficit (Liu et al., 2024). Our results suggest that WUE in rainfed wheat production could be improved by agronomic practices that includes matching of crop critical growth stages with ongoing rain spell as well as application of N in different rates and modification of source sink traits.

5. Conclusion

Our study highlighted the impact of source-sink modification under different N levels on crop phenology, leaf area, biomass, grain yield and N dynamics and it was well simulated by DSSAT_CERES-Wheat. The result showed that shading resulted to the reduction in crop phenology while spike halving treatments leads to increased (12 %) days to maturity as compared to control. Model simulation potential to generate accurate crop phenology could help crop mangers, agronomist and breeders to do accurate management and design new crop ideotypes under different sets of management and environments. Similarly, results can be used to have cultivars which can survive and provide sustainable yield under different RUE. Results pointed that source limitation shows more significant impact than sink limitation thus greater attention should be given to sources limitation in future so that we can have climate resilient cultivars. Similarly, Biomass-WUE and Grain-WUE in dryland agriculture could be improved through N fertilization and source sink manipulation. Finally, we conclude that higher source-sink ratio after anthesis can help crops to have higher capacity to avoid yield reduction due to abiotic and biotic stress.

Funding

This study was financially supported by Higher Education Commission of Pakistan through Grant HEC-NRPU-6132.

CRediT authorship contribution statement

Shakeel Ahmad: Writing – review & editing, Writing – original draft, Formal analysis, Conceptualization. **Mukhtar Ahmed:** Writing – review & editing, Writing – original draft, Supervision, Software, Resources, Methodology, Investigation, Funding acquisition, Formal analysis, Data curation, Conceptualization. **Muhammad Bilal:** Writing – original draft, Methodology, Investigation, Formal analysis, Data curation.

Declaration of Competing Interest

The authors declare that they have no known competing financial interests or personal relationships that could have appeared to influence the work reported in this paper.

Data availability

Data will be made available on request.

Acknowledgements

We acknowledge the contribution of co-authors and funding source.

References

Abbas, G., Ahmed, M., Fatima, Z., Hussain, S., Kheir, A.M.S., Ercişli, S., Ahmad, S., 2023. Modeling the potential impact of climate change on maize-maize cropping system in semi-arid environment and designing of adaptation options. Agric. For. Meteorol. 341, 109674.

Afzal, O., Ahmed, M., Fayyaz ul, H., Shabbir, G., Ahmed, S., Hoogenboom, G., 2024. CSM-CROPGRO model to simulate safflower phenological development and yield. Int J. Biometeorol. 68, 1213–1228.

Ahmad, S., Abbas, G., Ahmed, M., Fatima, Z., Anjum, M.A., Rasul, G., Khan, M.A., Hoogenboom, G., 2019. Climate warming and management impact on the change of phenology of the rice-wheat cropping system in Punjab, Pakistan. Field Crops Res. 230, 46–61.

Ahmed, M., 2020. Introduction to modern climate change, 2011, 252 pp, ISBN-10: 0521173159. In: Dessler, Andrew E. (Ed.), Science of The Total Environment, 734. Cambridge University Press.

Ahmed, M., 2023. The Science of Climate Change. In: Brinkmann, R. (Ed.), The Palgrave Handbook of Global Sustainability. Springer International Publishing, Cham, pp. 195–222.

Ahmed, M., Ahmad, S., Abbas, G., Hussain, S., Hoogenboom, G., 2024a. Cropping systems and application of models. Cropping Systems Modeling Under Changing Climate. Springer Nature Singapore, Singapore, pp. 1–22.
Ahmed, M., Ahmad, S., Abbas, G., Hussain, S., Hoogenboom, G., 2024b. Guar-Wheat System. Cropping Systems Modeling Under Changing Climate. Springer Nature Singapore, Singapore, pp. 411–430.
Ahmed, M., Akram, M.N., Asim, M., Aslam, M., Hassan, F.-u, Higgins, S., Stöckle, C.O., Hoogenboom, G., 2016. Calibration and validation of APSIM-Wheat and CERES-Wheat for spring wheat under rainfed conditions: models evaluation and application. Comput. Electron. Agric. 123, 384–401.
Ahmed, M., Fayyaz Ul, H., Van Ogtrop, F.F., 2014. Can models help to forecast rainwater dynamics for rainfed ecosystem? Weather Clim. Extrem. 5 (6), 48–55.
Ahmed, M., Rehman, A., Sarwar, N., Doğan, H., Abbas, G., Khan, M.A., Kan, M., Raza, M. A., Hussain, S., Ahmad, S., 2023. Deciding sowing-window for maize-based cropping system in arid and semiarid environments in Punjab, Pakistan. Turk. J. Agric. For. 47, 1078–1098.
Alonso, M.P., Abbate, P.E., Mirabella, N.E., Aramburu Merlos, F., Panelo, J.S., Pontaroli, A.C., 2018. Analysis of sink/source relations in bread wheat recombinant inbred lines and commercial cultivars under a high yield potential environment. Eur. J. Agron. 93, 82–87.
Álvaro, F., Royo, C., García del Moral, L., Villegas, D., 2008. Grain filling and dry matter translocation responses to source–sink modifications in a historical series of durum wheat. Crop Sci. 48, 1523–1531.
Amirhajloo, S., Gheysari, M., Shayannejad, M., Shirvani, M., 2023. Selection of the best nitrogen fertilizer management scenario in wheat based on Palmer drought severity index with an environmental perspective. Eur. J. Agron. 151, 126980.
Amouzou, K.A., Naab, J.B., Lamers, J.P.A., Becker, M., 2018. CERES-Maize and CERES-Sorghum for modeling growth, nitrogen and phosphorus uptake, and soil moisture dynamics in the dry savanna of West Africa. Field Crops Res. 217, 134–149.
Andarzian, B., Hoogenboom, G., Bannayan, M., Shirali, M., Andarzian, B., 2015. Determining optimum sowing date of wheat using CSM-CERES-Wheat model. J. Saudi Soc. Agric. Sci. 14, 189–199.
Anwar, M.R., Liu, D.L., Farquharson, R., Macadam, I., Abadi, A., Finlayson, J., Wang, B., Ramilan, T., 2015. Climate change impacts on phenology and yields of five broadacre crops at four climatologically distinct locations in Australia. Agric. Syst. 132, 133–144.
Arora, V.K., Singh, H., Singh, B., 2007. Analyzing wheat productivity responses to climatic, irrigation and fertilizer-nitrogen regimes in a semi-arid sub-tropical environment using the CERES-Wheat model. Agric. Wat. Manag. 94, 22–30.
Artru, S., Dumont, B., Ruget, F., Launay, M., Ripoche, D., Lassois, L., Garré, S., 2018. How does STICS crop model simulate crop growth and productivity under shade conditions? Field Crops Res. 215, 83–93.
Aslam, M.A., Ahmed, M., Stöckle, C.O., Higgins, S.S., Hassan, Fu, Hayat, R., 2017. Can growing degree days and photoperiod predict spring wheat phenology? Front. Environ. Sci. 5.
Asseng, S., Ewert, F., Rosenzweig, C., Jones, J.W., Hatfield, J.L., Ruane, A.C., Boote, K.J., Thorburn, P.J., Rotter, R.P., Cammarano, D., Brisson, N., Basso, B., Martre, P., Aggarwal, P.K., Angulo, C., Bertuzzi, P., Biernath, C., Challinor, A.J., Doltra, J., Gayler, S., Goldberg, R., Grant, R., Heng, L., Hooker, J., Hunt, L.A., Ingwersen, J., Izaurralde, R.C., Kersebaum, K.C., Muller, C., Naresh Kumar, S., Nendel, C., O/ 'Leary, G., Olesen, J.E., Osborne, T.M., Palosuo, T., Priesack, E., Ripoche, D., Semenov, M.A., Shcherbak, I., Steduto, P., Stockle, C., Stratonovitch, P., Streck, T., Supit, I., Tao, F., Travasso, M., Waha, K., Wallach, D., White, J.W., Williams, J.R., Wolf, J., 2013. Uncertainty in simulating wheat yields under climate change. Nat. Clim. Change 3, 827–832.
Asseng, S., Kassie, B.T., Labra, M.H., Amador, C., Calderini, D.F., 2016. Simulating the impact of source-sink manipulations in wheat. Field Crops Research.
Asseng, S., Kassie, B.T., Labra, M.H., Amador, C., Calderini, D.F., 2017. Simulating the impact of source-sink manipulations in wheat. Field Crops Res. 202, 47–56.
Asseng, S., Martre, P., Maiorano, A., Rötter, R.P., O'Leary, G.J., Fitzgerald, G.J., Girousse, C., Motzo, R., Giunta, F., Babar, M.A., Reynolds, M.P., Kheir, A.M.S., Thorburn, P.J., Waha, K., Ruane, A.C., Aggarwal, P.K., Ahmed, M., Balkovič, J., Basso, B., Biernath, C., Bindi, M., Cammarano, D., Challinor, A.J., De Sanctis, G., Dumont, B., Eyshi Rezaei, E., Fereres, E., Ferrise, R., Garcia-Vila, M., Gayler, S., Gao, Y., Horan, H., Hoogenboom, G., Izaurralde, R.C., Jabloun, M., Jones, C.D., Kassie, B.T., Kersebaum, K.-C., Klein, C., Koehler, A.-K., Liu, B., Minoli, S., Montesino San Martin, M., Müller, C., Naresh Kumar, S., Nendel, C., Olesen, J.E., Palosuo, T., Porter, J.R., Priesack, E., Ripoche, D., Semenov, M.A., Stöckle, C., Stratonovitch, P., Streck, T., Supit, I., Tao, F., Van der Velde, M., Wallach, D., Wang, E., Webber, H., Wolf, J., Xiao, L., Zhang, Z., Zhao, Z., Zhu, Y., Ewert, F., 2019. Climate change impact and adaptation for wheat protein. Glob. Change Biol. 25, 155–173.
Asseng, S., Turner, N., Keating, B.A., 2001. Analysis of water-and nitrogen-use efficiency of wheat in a Mediterranean climate. Plant Soil 233, 127–143.
Asseng, S., Van Herwaarden, A., 2003. Analysis of the benefits to wheat yield from assimilates stored prior to grain filling in a range of environments. Plant Soil 256, 217–229.
Asseng, S., Zhu, Y., Wang, E., Zhang, W., 2015. Chapter 20 - Crop modeling for climate change impact and adaptation A2 - Sadras. In: Victor, O., Calderini, D.F. (Eds.), Crop Physiology (Second Edition). Academic Press, San Diego, pp. 505–546.
Attia, A., Rajan, N., Xue, Q., Nair, S., Ibrahim, A., Hays, D., 2016. Application of DSSAT-CERES-Wheat model to simulate winter wheat response to irrigation management in the Texas High Plains. Agric. Water Manag. 165, 50–60.
Azmat, M., Ilyas, F., Sarwar, A., Huggel, C., Vaghefi, S.A., Hui, T., Qamar, M.U., Bilal, M., Ahmed, Z., 2021. Impacts of climate change on wheat phenology and yield in Indus Basin, Pakistan. Sci. Total Environ. 790, 148221.
Ban, H.-Y., Sim, D., Lee, K.-J., Kim, J., Kim, K.S., Lee, B.-W., 2015. Evaluating maize growth models "CERES-Maize" and "IXIM-Maize" under elevated temperature conditions. J. Crop Sci. Biotechnol. 18, 265–272.
Basso, B., Liu, L., Ritchie, J.T., 2016. A Comprehensive Review of the CERES-Wheat, -Maize and -Rice Models' Performances. In: Sparks, D.L. (Ed.), Advances in Agronomy. Academic Press, pp. 27–132.
Bongiovani, P.D.F., Frossard, E., de, S., Nóia Júnior, R., Asseng, S., Vuille-dit-Bille, N., Burton, A., Herrera, J.M., 2024. Responses of winter wheat genotypes to reduced rainfall, nitrogen fertilization and pre-crops in Switzerland. Field Crops Res. 308, 109272.
Borrás, L., Slafer, G.A., Otegui, Ma.E., 2004a. Seed dry weight response to source–sink manipulations in wheat, maize and soybean: a quantitative reappraisal. Field Crops Res. 86, 131–146.
Borrás, L., Slafer, G.A., Otegui, M.E., 2004b. Seed dry weight response to source–sink manipulations in wheat, maize and soybean: a quantitative reappraisal. Field Crops Res. 86, 131–146.
Borrill, P., Fahy, B., Smith, A.M., Uauy, C., 2015. Wheat Grain filling is limited by grain filling capacity rather than the duration of flag leaf photosynthesis: a case study using NAM RNAi plants. PLoS ONE 10, e0134947.
Bustos, D.V., Hasan, A.K., Reynolds, M.P., Calderini, D.F., 2013. Combining high grain number and weight through a DH-population to improve grain yield potential of wheat in high-yielding environments. Field Crops Res. 145, 106–115.
Cai, Z., Xie, T., Xu, J., 2021. Source–sink manipulations differentially affect carbon and nitrogen dynamics, fruit metabolites and yield of Sacha Inchi plants. BMC Plant Biol. 21, 160.
Cartelle, J., Pedró, A., Savin, R., Slafer, G.A., 2006. Grain weight responses to post-anthesis spikelet-trimming in an old and a modern wheat under Mediterranean conditions. Eur. J. Agron. 25, 365–371.
Chardon, X., Rigolot, C., Baratte, C., Espagnol, S., Raison, C., Martin-Clouaire, R., Rellier, J.P., Le Gall, A., Dourmad, J.Y., Piquemal, B., Leterme, P., Paillat, J.M., Delaby, L., Garcia, F., Peyraud, J.L., Poupa, J.C., Morvan, T., Faverdin, P., 2012. MELODIE: a whole-farm model to study the dynamics of nutrients in dairy and pig farms with crops. Animal 6, 1711–1721.
Cooper, M., Hammer, G.L., 1996. Plant adaptation and crop improvement. IRRI.
Dar, E.A., Brar, A.S., Mishra, S.K., Singh, K.B., 2017. Simulating response of wheat to timing and depth of irrigation water in drip irrigation system using CERES-Wheat model. Field Crops Res. 214, 149–163.
Deng, L., Zhang, H., Wang, C., Ma, W., Zhu, A., Zhang, F., Jiao, X., 2021. Improving the sustainability of the wheat supply chain through multi-stakeholder engagement. J. Clean. Prod. 321, 128837.
Dreccer, M.F., Fainges, J., Whish, J., Ogbonnaya, F.C., Sadras, V.O., 2018. Comparison of sensitive stages of wheat, barley, canola, chickpea and field pea to temperature and water stress across Australia. Agric. For. Meteorol. 248, 275–294.
Dueri, S., Brown, H., Asseng, S., Ewert, F., Webber, H., George, M., Craigie, R., Guarin, J. R., Pequeno, D.N.L., Stella, T., Ahmed, M., Alderman, P.D., Basso, B., Berger, A.G., Mujica, G.B., Cammarano, D., Chen, Y., Dumont, B., Rezaei, E.E., Fereres, E., Ferrise, R., Gaiser, T., Gao, Y., Garcia-Vila, M., Gayler, S., Hochman, Z., Hoogenboom, G., Kersebaum, K.C., Nendel, C., Olesen, J.E., Padovan, G., Palosuo, T., Priesack, E., Pullens, J.W.M., Rodríguez, A., Rötter, R.P., Ramos, M.R., Semenov, M.A., Senapati, N., Siebert, S., Srivastava, A.K., Stöckle, C., Supit, I., Tao, F., Thorburn, P., Wang, E., Weber, T.K.D., Xiao, L., Zhao, C., Zhao, J., Zhao, Z., Zhu, Y., Martre, P., 2022. Simulation of winter wheat response to variable sowing dates and densities in a high-yielding environment. J. Exp. Bot. 73, 5715–5729.
Enders, A., Vianna, M., Gaiser, T., Krauss, G., Webber, H., Srivastava, A.K., Seidel, S.J., Tewes, A., Rezaei, E.E., Ewert, F., 2023. SIMPLACE—a versatile modelling and simulation framework for sustainable crops and agroecosystems. silico Plants 5.
Fan, X., Li, Y., 2001. Effect of drought stress and drought tolerance heredity on nitrogen efficiency of winter wheat. Plant Nutrition. Springer, pp. 62–63.
Fang, H., Liu, F., Gu, X., Chen, P., Li, Y., Li, Y., 2022. The effect of source–sink on yield and water use of winter wheat under ridge-furrow with film mulching and nitrogen fertilization. Agric. Water Manag. 267, 107616.
Fang, Q., Zhang, H., He, J., Li, H., Wang, H., Li, D., Lv, X., Li, R., 2024. Water use strategies and shoot and root traits of high-yielding winter wheat cultivars under different water supply conditions, 14, 826.
Fatima, Z., Ahmed, M., Hussain, M., Abbas, G., Ul-Allah, S., Ahmad, S., Ahmed, N., Ali, M.A., Sarwar, G., Haque, Eu, Iqbal, P., Hussain, S., 2020. The fingerprints of climate warming on cereal crops phenology and adaptation options. Sci. Rep. 10, 18013.
Ferrante, A., Savin, R., Slafer, G.A., 2013. Is floret primordia death triggered by floret development in durum wheat? J. Exp. Bot. 64, 2859–2869.
Fu, J., Huang, Z., Wang, Z., Yang, J., Zhang, J.J.F.C.R., 2011. Pre-anthesis non-structural carbohydrate reserve in the stem enhances the sink strength of inferior spikelets during grain filling of rice, 123, 170–182.
Galmarini, S., Solazzo, E., Ferrise, R., Srivastava, A.K., Ahmed, M., Asseng, S., Cannon, A. J., Dentener, F., De Sanctis, G., Gaiser, T., Gao, Y., Gayler, S., Gutierrez, J.M., Hoogenboom, G., Iturbide, M., Jury, M., Lange, S., Loukos, H., Maraun, D., Moriondo, M., McGinnis, S., Nendel, C., Padovan, G., Riccio, A., Ripoche, D., Stockle, C.O., Supit, I., Thao, S., Trombi, G., Vrac, M., Weber, T.K.D., Zhao, C., 2024. Assessing the impact on crop modelling of multi- and uni-variate climate model bias adjustments. Agric. Syst. 215, 103846.
Gao, Y., Wallach, D., Liu, B., Dingkuhn, M., Boote, K.J., Singh, U., Asseng, S., Kahveci, T., He, J., Zhang, R., Confalonieri, R., Hoogenboom, G., 2020. Comparison of three calibration methods for modeling rice phenology. Agric. For. Meteorol. 280, 107785.
Gauvain, J.-L., Lee, C.-H., 1994. Maximum a posteriori estimation for multivariate Gaussian mixture observations of Markov chains. IEEE Trans. Speech Audio Process. 2, 291–298.

Gebbing, T., Schnyder, H., KÜhbauch, W., 1999. The utilization of pre-anthesis reserves in grain filling of wheat. Assessment by steady-state 13CO2/12CO2 labelling. Plant, Cell Environ. 22, 851–858.
González, F.G., Miralles, D.J., Slafer, G.A., 2011. Wheat floret survival as related to pre-anthesis spike growth. J. Exp. Bot. 62, 4889–4901.
González, F.G., Slafer, G.A., Miralles, D.J., 2003. Grain and floret number in response to photoperiod during stem elongation in fully and slightly vernalized wheats. Field Crops Res. 81, 17–27.
Gu, Y., Li, G., Sun, Y., Luo, W., Liu, X., Zhang, W., Qi, C., Zhao, Y., Tang, K., Zhang, Y., Shao, L., Xiong, Y., Si, C., Zhao, C., 2017. The effects of global dimming on the wheat crop grown in the Yangtze Basin of China simulated by SUCROS_LL, a process-based model. Ecol. Model. 350, 42–54.
Guarin, J.R., Martre, P., Ewert, F., Webber, H., Dueri, S., Calderini, D., Reynolds, M., Molero, G., Miralles, D., Garcia, G., Slafer, G., Giunta, F., Pequeno, D.N.L., Stella, T., Ahmed, M., Alderman, P.D., Basso, B., Berger, A.G., Bindi, M., Bracho-Mujica, G., Cammarano, D., Chen, Y., Dumont, B., Rezaei, E.E., Fereres, E., Ferrise, R., Gaiser, T., Gao, Y., Garcia-Vila, M., Gayler, S., Hochman, Z., Hoogenboom, G., Hunt, L.A., Kersebaum, K.C., Nendel, C., Olesen, J.E., Palosuo, T., Priesack, E., Pullens, J.W.M., Rodríguez, A., Rötter, R.P., Ramos, M.R., Semenov, M.A., Senapati, N., Siebert, S., Srivastava, A.K., Stöckle, C., Supit, I., Tao, F., Thorburn, P., Wang, E., Weber, T.K.D., Xiao, L., Zhang, Z., Zhao, C., Zhao, J., Zhao, Z., Zhu, Y., Asseng, S., 2022. Evidence for increasing global wheat yield potential. Environ. Res. Lett. 17, 124045.
Gui, Y.-W., Batool, A., El-Keblawy, A., Sheteiwy, M.S., Yang, Y.-M., Zhao, L., Duan, H.-X., Chang, S.-J., Xiong, Y.-C., 2024. Response of source-sink relationship to progressive water deficit in the domestication of dryland wheat. Plant Physiol. Biochem. 207, 108380.
Guo, Z., Chen, D., Schnurbusch, T., 2018. Plant and floret growth at distinct developmental stages during the stem elongation phase in wheat. Front. Plant Sci. 9.
Hafiza, B.S., Ishaque, W., Osman, R., Aziz, M., Ata-Ul-Karim, S.T., 2022. Simulation of wheat yield using CERES-Wheat under rainfed and supplemental irrigation conditions in a semi-arid environment. Agric. Water Manag. 264, 107510.
Heİdari, H., 2023. Alteration of wheat source-sink relation by nitrogen and spikelet removal. J. Tekirdag Agric. Fac. 20, 731–739.
Hussain, J., Khaliq, T., Ahmad, A., Akhtar, J., 2018. Performance of four crop model for simulations of wheat phenology, leaf growth, biomass and yield across planting dates. PLOS ONE 13, e0197546.
IBSNAT, 1988. International Benchmark Sites Network for Agrotechnology Transfer. The IBSNAT Decade. Department of Agronomy and Soil Science, College of Tropical Agriculture and Human Resources, University of Hawaii, Honoluly, Hawaii.
IPCC, 2023. Summary for Policymakers. In: Climate Change 2023: Synthesis Report. A Report of the Intergovernmental Panel on Climate Change. Contribution of Working Groups I, II and III to the Sixth Assessment Report of the Intergovernmental Panel on Climate Change [Core Writing Team, H. Lee and J. Romero (eds.)]. IPCC, Geneva, Switzerland, p. 36.
Ishaque, W., Osman, R., Hafiza, B.S., Malghani, S., Zhao, B., Xu, M., Ata-Ul-Karim, S.T., 2023. Quantifying the impacts of climate change on wheat phenology, yield, and evapotranspiration under irrigated and rainfed conditions. Agric. Water Manag. 275, 108017.
Jahan, M.A.H.S., Sen, R., Ishtiaque, S., Choudhury, A.K., Akhter, S., Ahmed, F., Biswas, J. C., Manirruzaman, M., Miah, M.M., Rahman, M.M., Kalra, N., 2018. Optimizing sowing window for wheat cultivation in Bangladesh using CERES-wheat crop simulation model. Agric., Ecosyst. Environ. 258, 23–29.
Jones, J.W., Hoogenboom, G., Porter, C.H., Boote, K.J., Batchelor, W.D., Hunt, L.A., Wilkens, P.W., Singh, U., Gijsman, A.J., Ritchie, J.T., 2003. The DSSAT cropping system model. Eur. J. Agron. 18, 235–265.
Kephe, P.N., Ayisi, K.K., Petja, B.M., 2021. Challenges and opportunities in crop simulation modelling under seasonal and projected climate change scenarios for crop production in South Africa. Agric. Food Secur. 10, 10.
Kheir, A.M.S., El Baroudy, A., Aiad, M.A., Zoghdan, M.G., Abd El-Aziz, M.A., Ali, M.G.M., Fullen, M.A., 2019. Impacts of rising temperature, carbon dioxide concentration and sea level on wheat production in North Nile delta. Sci. Total Environ. 651, 3161–3173.
Kimball, B.A., Thorp, K.R., Boote, K.J., Stockle, C., Suyker, A.E., Evett, S.R., Brauer, D.K., Coyle, G.G., Copeland, K.S., Marek, G.W., Colaizzi, P.D., Acutis, M., Alimagham, S., Archontoulis, S., Babacar, F., Barcza, Z., Basso, B., Bertuzzi, P., Constantin, J., De Antoni Migliorati, M., Dumont, B., Durand, J.-L., Fodor, N., Gaiser, T., Garofalo, P., Gayler, S., Giglio, L., Grant, R., Guan, K., Hoogenboom, G., Jiang, Q., Kim, S.-H., Kisekka, I., Lizaso, J., Masia, S., Meng, H., Mereu, V., Mukhtar, A., Perego, A., Peng, B., Priesack, E., Qi, Z., Shelia, V., Snyder, R., Soltani, A., Spano, D., Srivastava, A., Thomson, A., Timlin, D., Trabucco, A., Webber, H., Weber, T., Willaume, M., Williams, K., van der Laan, M., Ventrella, D., Viswanathan, M., Xu, X., Zhou, W., 2023. Simulation of evapotranspiration and yield of maize: an inter-comparison among 41 maize models. Agric. For. Meteorol. 333, 109396.
Kiniry, J.R., Tischler, C.R., Rosenthal, W.D., Gerik, T.J., 1992. Nonstructural carbohydrate utilization by sorghum and maize shaded during grain growth. Crop Sci. 32, 131–137.
Lázaro, L., Abbate, P., Cogliatti, D., Andrade, F., 2010. Relationship between yield, growth and spike weight in wheat under phosphorus deficiency and shading. J. Agric. Sci. 148, 83–93.
Lee, C.-C., Zeng, M., Luo, K., 2024. How does climate change affect food security? Evidence from China. Environ. Impact Assess. Rev. 104, 107324.
Li, H., Shao, L., Liu, X., Sun, H., Chen, S., Zhang, X., 2023. What matters more, biomass accumulation or allocation, in yield and water productivity improvement for winter wheat during the past two decades. Eur. J. Agron. 149, 126910.
Liu, X., Yin, B., Bao, X., Hou, X., Wang, T., Shang, C., Yang, M., Zhen, W., 2024. Optimization of irrigation period improves wheat yield by regulating source-sink relationship under water deficit. Eur. J. Agron. 156, 127164.
Lv, X., Zhang, Y., Zhang, Y., Fan, S., Kong, L., 2020. Source-sink modifications affect leaf senescence and grain mass in wheat as revealed by proteomic analysis. BMC Plant Biol. 20, 257.
Mahakosee, S., Jogloy, S., Vorasoot, N., Theerakulpisut, P., Toomsan, B., Holbrook, C.C., Kvien, C.K., Banterng, P., 2022. Light interception and radiation use efficiency of three cassava genotypes with different plant types and seasonal variations. Agronomy 12, 2888.
Matthews, R.B., Rivington, M., Muhammed, S., Newton, A.C., Hallett, P.D., 2013. Adapting crops and cropping systems to future climates to ensure food security: the role of crop modelling. Glob. Food Secur. 2, 24–28.
Menzel, A., Yuan, Y., Matiu, M., Sparks, T., Scheifinger, H., Gehrig, R., Estrella, N., 2020. Climate change fingerprints in recent European plant phenology. Glob. Change Biol. 26, 2599–2612.
Miralles, D., Slafer, G.A., 2007a. Sink limitations to yield in wheat: how could it be reduced? J. Agric. Sci.-Camb.- 145, 139.
Miralles, D.J., Slafer, G.A., 2007b. Sink limitations to yield in wheat: how could it be reduced? J. Agric. Sci. vol. 145 (núm. 2), 139–149, 2007.
Mohan, N., Jhandai, S., Bhadu, S., Sharma, L., Kaur, T., Saharan, V., Pal, A., 2023. Acclimation response and management strategies to combat heat stress in wheat for sustainable agriculture: a state-of-the-art review. Plant Sci. 336, 111834.
Monzon, J.P., Sadras, V.O., Abbate, P.A., Caviglia, O.P., 2007. Modelling management strategies for wheat–soybean double crops in the south-eastern Pampas. Field Crops Res. 101, 44–52.
Naz, S., Ahmed, M., Abbas, G., Fatima, Z., Hussain, S., Iqbal, P., Ghani, A., Ali, M., Awan, T.H., Samad, N., Aasim, M., Ercisli, S., Ahmad, S., 2024. Assessment of climate change impact on potato-potato cropping system under semi-arid environment and designing of adaptation strategies. Potato Res.
Pasley, H., Wenham, K., Bell, L., Huth, N., Holzworth, D., Chaki, A., Gaydon, D., Collins, M., 2023. APSIM next generation mungbean model: a tool for advancing mungbean production. Field Crops Res. 298, 108955.
Ponsioen, T.C., Yin, X., Spiertz, J.H.J., Royo, C., 2007. Effects of Abiotic Stress on Sink and Source Affecting Grain Yield and Quality of Durum Wheat: A Model Evaluation. Springer Netherlands, Dordrecht, pp. 633–639.
Potgieter, A.B., Zhao, Y., Zarco-Tejada, P.J., Chenu, K., Zhang, Y., Porker, K., Biddulph, B., Dang, Y.P., Neale, T., Roosta, F., Chapman, S., 2021. Evolution and application of digital technologies to predict crop type and crop phenology in agriculture. silico Plants 3.
Rafique, R., Ahmad, T., Ahmed, M., Khan, M.A., 2024. Adapting the process based STICS model to simulate phenology and yield of table grapes- a high value fruit crop in a new emerging viticulture zone of South Asia. Sci. Hortic. 336, 113419.
Ram, H., Dadhwal, V., Vashist, K.K., Kaur, H., 2013. Grain yield and water use efficiency of wheat (Triticum aestivum L.) in relation to irrigation levels and rice straw mulching in North West India. Agric. Water Manag. 128, 92–101.
Reynolds, M., Calderini, D., Condon, A., Vargas, M., 2007. Association of source/sink traits with yield, biomass and radiation use efficiency among random sister lines from three wheat crosses in a high-yield environment.
Reynolds, M., Pellegrineschi, A., Skovmand, B., 2005. Sink-limitation to yield and biomass: a summary of some investigations in spring wheat. Ann. Appl. Biol. 146, 39–49.
Rezaei, E.E., Siebert, S., Ewert, F., 2015. Intensity of heat stress in winter wheat—phenology compensates for the adverse effect of global warming. Environ. Res. Lett. 10, 024012.
Ritchie, J.T., Singh, U., Godwin, D.C., Bowen, W.T., 1998. Cereal growth, development and yield. In: Tsuji, G., Hoogenboom, G., Thornton, P. (Eds.), Understanding Options for Agricultural Production. Springer Netherlands, pp. 79–98.
Salcedo, G., 2015. DairyCant: a model for the reduction of dairy farm greenhouse gas emissions. Adv. Anim. Biosci. 6, 26–28.
Schnyder, H., 1993. The role of carbohydrate storage and redistribution in the source-sink relations of wheat and barley during grain filling-a review. N. Phytol. 123, 233–245.
Serrago, R.A., Alzueta, I., Savin, R., Slafer, G.A., 2013. Understanding grain yield responses to source–sink ratios during grain filling in wheat and barley under contrasting environments. Field Crops Res. 150, 42–51.
Shewry, P.R., Hey, S.J., 2015. The contribution of wheat to human diet and health. Food Energy Secur. 4, 178–202.
Sinclair, T., Jamieson, P., 2006. Grain number, wheat yield, and bottling beer: an analysis. Field Crops Res. 98, 60–67.
Singh, P.K., Singh, K.K., Baxla, A.K., Rathore, L.S., 2015. Impact of Climatic Variability on Wheat Yield Predication using DSSAT v 4.5 (CERES-Wheat) Model for the different Agroclimatic zones in India. In: Singh, A.K., Dagar, J.C., Arunachalam, A., R, G., Shelat, K.N. (Eds.), Climate Change Modelling, Planning and Policy for Agriculture. Springer India, pp. 45–55.
Slafer, G.A., Savin, R., 1994. Source—sink relationships and grain mass at different positions within the spike in wheat. Field Crops Res. 37, 39–49.
Sun, J., Yang, L., Wang, Y., Ort, D.R., 2009. FACE-ing the global change: opportunities for improvement in photosynthetic radiation use efficiency and crop yield. Plant Sci. 177, 511–522.
Uddling, J., Gelang-Alfredsson, J., Karlsson, P.E., Selldén, G., Pleijel, H., 2008. Source–sink balance of wheat determines responsiveness of grain production to increased [CO 2] and water supply. Agric. Ecosyst. Environ. 127, 215–222.
van Ogtrop, F., Ahmad, M., Moeller, C., 2014. Principal components of sea surface temperatures as predictors of seasonal rainfall in rainfed wheat growing areas of Pakistan. Meteorol. Appl. 21, 431–443.

Wallach, D., Palosuo, T., Thorburn, P., Seidel, S.J., Gourdain, E., Asseng, S., Basso, B., Buis, S., Crout, N.M.J., Dibari, C., Dumont, B., Ferrise, R., Gaiser, T., Garcia, C., Gayler, S., Ghahramani, A., Hochman, Z., Hoek, S., Horan, H., Hoogenboom, G., Huang, M., Jabloun, M., Jing, Q., Justes, E., Kersebaum, K.C., Klosterhalfen, A., Launay, M., Luo, Q., Maestrini, B., Mielenz, H., Moriondo, M., Nariman Zadeh, H., Olesen, J.E., Poyda, A., Priesack, E., Pullens, J.W.M., Qian, B., Schütze, N., Shelia, V., Souissi, A., Specka, X., Srivastava, A.K., Stella, T., Streck, T., Trombi, G., Wallor, E., Wang, J., Weber, T.K.D., Weihermüller, L., de Wit, A., Wöhling, T., Xiao, L., Zhao, C., Zhu, Y., 2019. How well do crop models predict phenology, with emphasis on the effect of calibration. bioRxiv, 708578.
Wallach, D., Palosuo, T., Thorburn, P., Mielenz, H., Buis, S., Hochman, Z., Gourdain, E., Andrianasolo, F., Dumont, B., Ferrise, R., Gaiser, T., Garcia, C., Gayler, S., Harrison, M., Hiremath, S., Horan, H., Hoogenboom, G., Jansson, P.-E., Jing, Q., Justes, E., Kersebaum, K.-C., Launay, M., Lewan, E., Liu, K., Mequanint, F., Moriondo, M., Nendel, C., Padovan, G., Qian, B., Schütze, N., Seserman, D.-M., Shelia, V., Souissi, A., Specka, X., Srivastava, A.K., Trombi, G., Weber, T.K.D., Weihermüller, L., Wöhling, T., Seidel, S.J., 2023. Proposal and extensive test of a calibration protocol for crop phenology models. Agron. Sustain. Dev. 43, 46.
Wang, E., Engel, T., 1998. Simulation of phenological development of wheat crops. Agric. Syst. 58, 1–24.
Wang, Q., Li, F., Zhao, L., Zhang, E., Shi, S., Zhao, W., Song, W., Vance, M.M., 2010. Effects of irrigation and nitrogen application rates on nitrate nitrogen distribution and fertilizer nitrogen loss, wheat yield and nitrogen uptake on a recently reclaimed sandy farmland. Plant Soil 337, 325–339.
Wang, B., Liu, D.L., Asseng, S., Macadam, I., Yu, Q., 2015. Impact of climate change on wheat flowering time in eastern Australia. Agric. For. Meteorol. 209–210, 11–21.
Wang, Y., Peng, Y., Lin, J., Wang, L., Jia, Z., Zhang, R., 2023. Optimal nitrogen management to achieve high wheat grain yield, grain protein content, and water productivity: a meta-analysis. Agric. Water Manag. 290, 108587.
Warraich, E., Ahmad, N., Basra, S., Afzal, I., 2002. Effect of nitrogen on source-sink relationship in wheat. Int. J. Agric. Biol. 4, 300–302.
White, J.W., Hoogenboom, G., Kimball, B.A., Wall, G.W., 2011. Methodologies for simulating impacts of climate change on crop production. Field Crops Res. 124, 357–368.
Willmott, C.J., 1981. On the validation of models. Phys. Geogr. 2, 184–194.
Xiao-li, W.U., Miao, L.I.U., Chao-su, L.I., McHugh, A.D., Ming, L.I., Tao, X., Yu-bin, L.I.U., Yong-lu, T., 2022. Source–sink relations and responses to sink–source manipulations during grain filling in wheat. J. Integr. Agric. 21, 1593–1605.
Xu, C., Tao, H., Tian, B., Gao, Y., Ren, J., Wang, P., 2016. Limited-irrigation improves water use efficiency and soil reservoir capacity through regulating root and canopy growth of winter wheat. Field Crops Res. 196, 268–275.
Yan, W., Wallace, D.H., 1998. Simulation and prediction of plant phenology for five crops based on photoperiod×temperature interaction. Ann. Bot. 81, 705–716.
Yang, X., Asseng, S., Wong, M.T.F., Yu, Q., Li, J., Liu, E., 2013. Quantifying the interactive impacts of global dimming and warming on wheat yield and water use in China. Agric. For. Meteorol. 182–183 342–351.
Yu, Y., Cheng, Q., Wang, F., Zhu, Y., Shang, X., Jones, A., He, H., Song, Y., 2023. Crop/plant modeling supports plant breeding: i. optimization of environmental factors in accelerating crop growth and development for speed breeding. Plant Phenomics 5, 0099.
Zahra, N., Wahid, A., Hafeez, M.B., Ullah, A., Siddique, K.H.M., Farooq, M., 2021. Grain development in wheat under combined heat and drought stress: plant responses and management. Environ. Exp. Bot. 188, 104517.
Zeng, H., Jia, G., Epstein, H., 2011. Recent changes in phenology over the northern high latitudes detected from multi-satellite data. Environ. Res. Lett. 6, 045508.
Zhang, H., Turner, N.C., Poole, M.L., 2010. Source–sink balance and manipulating sink–source relations of wheat indicate that the yield potential of wheat is sink-limited in high-rainfall zones. Crop Pasture Sci. 61, 852–861.